

# How Pomerons Meet in Coloured Glass

Carlo Ewerz <sup>a</sup>, Volker Schatz <sup>b</sup>

*Institut für Theoretische Physik, Universität Heidelberg  
Philosophenweg 16, D-69120 Heidelberg, Germany*

## Abstract

We compute the perturbative one-to-three Pomeron vertex in the colour glass condensate using the extended generalized leading logarithmic approximation in high energy QCD. The vertex is shown to be a conformal four-point function in two-dimensional impact parameter space. Our result indicates the inequivalence of different approaches to the problem of describing the colour glass condensate.

---

<sup>a</sup> email: C.Ewerz@thphys.uni-heidelberg.de

<sup>b</sup> email: V.Schatz@thphys.uni-heidelberg.de

# 1 Introduction

In hadronic collisions at high energy the partons inside the colliding hadrons form a very dense system which is known as the colour glass condensate. The colour glass condensate is expected to have very interesting properties which can be studied experimentally in deep inelastic lepton-hadron scattering as well as in hadron-hadron collisions. One aspect of particular interest is the question whether the parton densities inside the colliding hadrons saturate at sufficiently high energies. If saturation indeed takes place it can in turn tame the growth of hadronic cross sections with the centre-of-mass energy  $\sqrt{s}$ . It is a very challenging theoretical problem to determine the relevant scales in the energy and in the momentum transfer at which saturation effects set in and to predict the resulting behaviour of the cross sections.

A variety of different approaches has been developed in order to find answers to these questions. The approach which has been most popular recently and from which the name colour glass condensate originates is the one initiated by McLerran and Venu-gopalan [1, 2, 3] which was further developed for example in [4, 5, 6], for a review and further references see [7]. A related approach based on the operator expansion method applied to Wilson line operators was used in [8]-[12]. The relation between these two approaches was established in [13]. The latter approach leads to a hierarchy of equations which can be drastically simplified in the large- $N_c$  limit. In this limit one obtains the so-called Balitsky-Kovchegov equation which has also been obtained in [14] using the colour dipole approach to high energy scattering [15]-[18]. In the colour dipole approach one studies the evolution of a small colour dipole due to gluon emissions. In the large- $N_c$  limit the emission of a gluon can be interpreted as a splitting of the dipole into two dipoles, and the interaction of two such systems after evolution is described by the basic dipole-dipole scattering via gluon exchange.

Another approach to the physics of the colour glass condensate is the classic one based on the perturbative resummation of large logarithms of the centre-of-mass energy  $\sqrt{s}$  in high energy collisions. This resummation program was performed in [19, 20], resulting in the celebrated Balitsky-Fadin-Kuraev-Lipatov (BFKL) equation which resums all terms of the form  $(\alpha_s \log s)^n$  in the perturbative series. This approximation scheme is called the leading logarithmic approximation (LLA). On the level of the cross section, i. e. the squared amplitude, the BFKL equation describes the exchange of two interacting reggeised gluons in the  $t$ -channel, called the BFKL Pomeron. It is known that at higher energies exchanges of more than two gluons in the  $t$ -channel eventually become important, and one has to include them in order to find an appropriate description of the high energy limit. This is done in the generalized leading logarithmic approximation (GLLA). There are two forms of this approximation. The first one considers only exchanges in which the number of reggeised gluons remains constant during the  $t$ -channel evolution. The corresponding resummation of the leading logarithmic terms for a given number of gluons is encoded in the Bartels-Kwieciński-Praszałowicz (BKP) equations [21, 22]. That form of the GLLA can be considered as the quantum mechanics of states of  $n$  gluons exchanged in the  $t$ -channel. One expects to obtain a scattering amplitude satisfying the unitarity bound for the total cross section when all contributions with arbitrary  $n$  are included<sup>1</sup>. In order to obtain amplitudes satis-

---

<sup>1</sup>Therefor the  $n$ -gluon amplitudes of both versions of the GLLA are often called unitarity corrections.

fying unitarity also in all subchannels one has to include also contributions in which the number of reggeised gluons is permitted to vary during the  $t$ -channel evolution, giving rise to the second version of the GLLA which we call extended GLLA (EGLLA) [21, 23, 24]. That step turns the quantum mechanical problem of states with a fixed number of gluons into a quantum field theory of reggeised gluons in which states with different numbers of gluons are coupled to each other. The corresponding amplitudes are described by a tower of coupled integral equations generalizing the BKP equations. These equations constitute the basis of the EGLLA. Their structure has been investigated in a series of papers, see for example [25]-[35]. A remarkable result found in these studies is the conformal invariance of the amplitudes of the EGLLA in two-dimensional impact parameter space. There are in fact strong indications that the whole set of amplitudes can be formulated as a conformal field theory.

The approaches mentioned above are to a large extent based on the application of perturbative concepts. The use of perturbation theory is justified in high energy scattering processes which are dominated by a single large momentum scale. It would clearly be a great success if one could obtain a good description of the high energy limit of QCD in a perturbative framework. The practical applicability of such a perturbative picture would remain restricted to certain scattering processes dominated by a large momentum scale. Nevertheless, it would be very valuable to see how for example the structure of Regge theory can emerge from perturbative QCD. It should be emphasized, however, that the wealth of hadronic scattering processes at high energies is dominated by low momenta. A satisfactory description of high energy scattering therefore eventually requires to include nonperturbative effects. The hope is that one can explore the transition region to low momenta starting from the perturbative framework. A recent example for the use of this method is [36] where it was found that the validity of the Froissart bound on the high energy behaviour of total cross sections,  $\sigma_T \leq \text{const} \cdot \log s$ , appears to be closely related to confinement effects. In the long-term perspective one would hope that it is also possible to find relations between the perturbative approaches and generically nonperturbative approaches to high energy scattering like for example the implementation [37]-[40] of the stochastic vacuum model of [41, 42, 43] in the non-perturbative framework of [44], or even Regge theory (see for example [45]), although this is extremely challenging.

The different perturbatively motivated approaches have their respective advantages. The approach of [1]-[7] is for example particularly well suited for estimating the momentum scales at which saturation effects set in whereas in the EGLLA the conformal invariance of the amplitudes and the phenomenon of reggeisation become particularly transparent. It would obviously be very desirable to understand the exact relations between these different approaches to the problem of high energy scattering. Interestingly, the BFKL equation is reproduced by all approaches mentioned above in a suitable limit corresponding to sufficiently low parton densities. In particular, that limit corresponds to a situation in which nonlinear effects in the evolution of the system can be neglected. Another important quantity which plays an important role in all approaches to the colour glass condensate is the perturbative one-to-two Pomeron vertex which was first derived in the EGLLA [27, 29]. Its value for the leading Pomeron states was computed in [46] and was found to agree with the value found in the dipole model of high energy scattering [47, 48]. The very same vertex occurs also in the other approaches and is a crucial ingredient for example in the Balitsky-Kovchegov equation.

In order to find characteristic differences between the different approaches one should therefore go beyond the approximation in which only Pomerons and their simplest vertex occurs. One possibility is to look at the exchange of negative charge parity quantum numbers associated with the Odderon, for a review see [49]. So far, the Odderon has only been identified and studied in the two versions of the GLLA. The other promising possibility is to study vertices with more than three Pomerons and here in particular the one-to-three Pomeron vertex. This vertex has so far only been considered in the dipole model, and there are apparently contradicting findings about its existence in the literature [30, 50]. In the present paper we derive the one-to-three Pomeron vertex in the colour glass condensate and hence prove the existence of such a vertex. We use the framework of the EGLLA to obtain the vertex by projecting the two-to-six reggeised gluon vertex calculated in [31] onto Pomeron eigenfunctions.

The paper is organised as follows. In section 2 we recall some important properties of the EGLLA and describe in particular the effective two-to-six reggeon vertex. We also discuss the main results for the one-to-two Pomeron vertex and the available results and conjectures concerning vertices with more Pomerons. We describe how the effective reggeon vertices of the EGLLA can be used to calculate multi-Pomeron vertices, in particular how the one-to-three Pomeron vertex is obtained from the two-to-six reggeon vertex. In section 3 we perform the explicit calculation of the one-to-three Pomeron vertex. Collecting the different contributions obtained in that section we give our final result for the one-to-three Pomeron vertex and discuss its implications in section 4. Some useful formulae needed for the calculation are derived in the appendix.

## 2 Extended GLLA, effective reggeised gluon vertices and Pomeron vertices

### 2.1 Extended GLLA

In the EGLLA one considers exchanges in the  $t$ -channel in which the number of reggeised gluons can fluctuate during the  $t$ -channel evolution. The objects of interest in the EGLLA are amplitudes describing the production of  $n$  reggeised gluons in the  $t$ -channel. For any given  $n$  one then resums all diagrams of the perturbative series which contain the maximal number of logarithms of the energy for that  $n$ . So far the EGLLA has been studied explicitly only for the case that the system of reggeised gluons is coupled to a virtual photon impact factor. It is expected that due to high energy factorization the results obtained in that special case are universal. In particular, the interaction vertices between states with different numbers of reggeised gluons have a universal meaning independent of the impact factor.

The amplitudes  $D_n^{a_1 \dots a_n}(\mathbf{k}_1, \dots, \mathbf{k}_n)$  describe the production of  $n$  reggeised gluons in the  $t$ -channel carrying transverse momenta  $\mathbf{k}_i$  and colour labels  $a_i$ . The lowest order term of these amplitudes is given by the virtual photon impact factor consisting of a quark loop to which the  $n$  gluons are coupled. But there are also terms in which less than  $n$  gluons are coupled to the quark loop and there are transitions to more gluons during the  $t$ -channel evolution. Technically this means that the amplitudes  $D_n$  obey a tower of coupled integral equations in which the equation for a given  $n$  involves all amplitudes  $D_m$  with  $m < n$ . The first of these integral equations (i.e. the one for

$D_2$ ) is identical to the BFKL equation. In the higher equations new transition kernels occur which are generalizations of the BFKL kernel. They have been derived in [24]. Various aspects of the system of the integral equations have been studied in [25]-[35], for a detailed description and a systematic approach to solving the equations see [31].

The structure of the solutions is such that they involve only states with fixed even numbers of gluons which are coupled to each other by effective transition vertices that can be computed explicitly. The reggeisation of the gluon is responsible for the fact that in the solutions of the integral equations for the amplitudes  $D_n$  the states with fixed odd numbers of gluons do not occur. The simplest example for reggeisation in the amplitudes is the three-gluon amplitude which can be shown to be a superposition of two-gluon amplitudes of the form

$$D_3^{abc}(\mathbf{k}_1, \mathbf{k}_2, \mathbf{k}_3) = gf_{abc} [D_2(\mathbf{k}_1 + \mathbf{k}_2, \mathbf{k}_3) - D_2(\mathbf{k}_1 + \mathbf{k}_3, \mathbf{k}_2) + D_2(\mathbf{k}_1, \mathbf{k}_2 + \mathbf{k}_3)] . \quad (1)$$

As a consequence, an actual three-gluon state in the  $t$ -channel does not occur. In each of the three terms in this expression the momenta of two gluons enter only as a sum. They can be regarded as forming a ‘more composite’ reggeised gluon that occurs in the amplitude  $D_2$ . Reggeisation occurs also in all higher amplitudes  $D_n$ , all of which contain a contribution which can be decomposed into two-gluon amplitudes in a way similar to (1). In the higher amplitudes also more than two gluons can form a more composite reggeised gluon. The details of this process are discussed in [33].

The three-gluon amplitude can be written completely in terms of two-gluon amplitudes. In the higher amplitudes with  $n \geq 4$  gluons additional contributions occur. The structure of the four-gluon amplitude can be written in symbolic form as [26, 27]:

$$D_4 = \sum \left[ \text{diagram 1} \right] + \left[ \text{diagram 2} \right] V_{2 \rightarrow 4} . \quad (2)$$

Here the first term is again the reggeising part consisting of a superposition of two-gluon amplitudes in a way similar to (1). In the second term the  $t$ -channel evolution starts with a two-gluon state that is coupled to a full four-gluon state via a new effective 2-to-4 gluon transition vertex  $V_{2 \rightarrow 4}$  the explicit form of which was found in [26, 27]. As can be seen from (2) the four-gluon state does not couple directly to the quark box diagram of the photon impact factor.

The structure emerging here is that of a quantum field theory in which states with different numbers of gluons are coupled to each other via effective transition vertices like  $V_{2 \rightarrow 4}$ . This structure has been shown to persist also to higher amplitudes in [31]. There the amplitudes with up to six gluons were studied. It turns out that the five-gluon amplitude can be written completely in terms of two-gluon amplitudes and four-gluon amplitudes containing the vertex  $V_{2 \rightarrow 4}$ . The mechanism of reggeisation is universal and it is expected that all amplitudes  $D_n$  with an odd number  $n$  of gluons are superpositions of lower amplitudes with even numbers of gluons. The six-gluon amplitude  $D_6$  was shown to consist of two reggeising parts, being superpositions of two- and four-gluon

amplitudes, and a part in which a two-gluon state is coupled to a six-gluon state via a new effective transition vertex  $V_{2 \rightarrow 6}$  which has been computed explicitly in [31]. This vertex will be the starting point for our calculation of the one-to-three Pomeron vertex. We therefore want to describe it in more detail now. Closing this section we point out that the effective transition vertices have the remarkable property of being conformally invariant in two-dimensional impact parameter space [28, 34].

## 2.2 The $2 \rightarrow 6$ reggeised gluon vertex

Let us now review the properties of the two-to-six reggeised gluon vertex occurring in the effective field theory structure found for the  $n$ -gluon amplitudes  $D_n$ . Here we concentrate on the properties which are essential for the calculation of the one-to-three Pomeron vertex, for the derivation and further properties of the two-to-six gluon vertex we refer the reader to [31, 34].

The two-to-six vertex couples a two-gluon state to a six-gluon state. The two-gluon state is given by a BFKL Pomeron amplitude. In [31] only the case was considered in which that Pomeron amplitude is coupled to a quark loop. The corresponding Pomeron amplitude is denoted by  $D_2$ . Further below we will instead use a Pomeron amplitude  $\Phi_2$  without the quark loop and then assume it to be an eigenfunction of the BFKL kernel. The two-to-six vertex is defined as an integral operator acting on the two-gluon state  $D_2$ . It carries six colour labels for the outgoing gluons, and the incoming gluons are in a colour singlet state. Further the vertex is a function of the transverse momenta of the incoming and outgoing gluons. When the vertex acts on the two-gluon state  $D_2$  one integrates over the transverse momenta of the two incoming gluons. We will use a shorthand notation in which the six momentum arguments are replaced by the indices of the respective gluons,

$$(V_{2 \rightarrow 6}^{a_1 a_2 a_3 a_4 a_5 a_6} D_2)(\mathbf{k}_1, \mathbf{k}_2, \mathbf{k}_3, \mathbf{k}_4, \mathbf{k}_5, \mathbf{k}_6) = (V_{2 \rightarrow 6}^{a_1 a_2 a_3 a_4 a_5 a_6} D_2)(1, 2, 3, 4, 5, 6), \quad (3)$$

i.e. 1 stands for  $\mathbf{k}_1$ , 2 for  $\mathbf{k}_2$  and so on. A string of several indices, for instance 123, means the sum of the momenta,  $\mathbf{k}_1 + \mathbf{k}_2 + \mathbf{k}_3$ . An empty argument, which will be denoted by “—”, stands for zero momentum. This notation has the advantage that it can be easily transformed into a configuration-space expression. In configuration space, an index stands for the corresponding coordinate. A string of indices means that the coordinates are identified via two-dimensional delta functions by which the expression has to be multiplied. An empty argument “—” translates into an integral over the corresponding coordinate argument in position space.

The dependence of the vertex on the colour labels of the six outgoing gluons is given by

$$\begin{aligned} (V_{2 \rightarrow 6}^{a_1 a_2 a_3 a_4 a_5 a_6} D_2)(1, 2, 3, 4, 5, 6) = & d_{a_1 a_2 a_3} d_{a_4 a_5 a_6} (W D_2)(1, 2, 3; 4, 5, 6) \\ & + d_{a_1 a_2 a_4} d_{a_3 a_5 a_6} (W D_2)(1, 2, 4; 3, 5, 6) + \dots \end{aligned} \quad (4)$$

It contains only colour tensors which are products of two symmetric structure constants  $d_{abc}$  of  $su(3)$ . The sum runs over all ten partitions of the six momenta and the corresponding colour indices into two groups of three.

The function  $(W D_2)$  is a convolution of a function  $W$  and a Pomeron amplitude  $D_2$ . As we have already pointed out the vertex occurs only in situations in which it

acts on a BFKL Pomeron state, and we will therefore consider only the combination  $(WD_2)$  rather than the integral operator  $W$  alone. Note that the function  $(WD_2)$  is the same in all terms in (4), only the momentum arguments are permuted in the different terms. As shown in [34] the function  $(WD_2)$  can be expressed in terms of a function  $G$ ,

$$(WD_2)(1, 2, 3; 4, 5, 6) = \frac{g^4}{8} \sum_{M \in \mathcal{P}(\{1, \dots, 6\})} (-1)^{\#M} G(123 \setminus M, M, 456 \setminus M). \quad (5)$$

This sum runs over all subsets  $M$  of the set of indices. The notation “ $123 \setminus M$ ” means the indices 1, 2 and 3 except those contained in  $M$ .  $\#M$  is the number of indices contained in  $M$ . This sum and the symmetry of the function  $G$  under exchange of its first and third argument cause the function  $(WD_2)$  to be symmetric under all permutations of its first three and its last three arguments, and under exchange of these two groups of arguments. Together with the sum in (4), this makes the  $2 \rightarrow 6$  vertex symmetric under arbitrary permutations of the six outgoing gluons, i. e. under simultaneous permutations of the colour labels and momenta of the gluons.

The function  $G$  had been introduced in [27] and was further analysed in [30, 35]. It depends on three momentum arguments and has the following form:

$$G(1, 2, 3) = \frac{g^2}{2} [2c(123) - 2b(12, 3) - 2b(23, 1) + 2a(2, 1, 3) + t(12, 3) + t(23, 1) - s(2, 1, 3) - s(2, 3, 1)], \quad (6)$$

with component functions  $a$ ,  $b$ ,  $c$ ,  $s$ , and  $t$  which will be defined below. It can be easily seen already from (6) that  $G$  is symmetric under the exchange of its first and third argument. That symmetry does not apply to the second argument. However, there is a different interesting property related to that argument. When the second momentum argument is set to zero, the  $a$  and  $s$  functions vanish and  $G$  essentially reduces to the well-known BFKL kernel applied the amplitude  $D_2$ ,

$$\begin{aligned} G(1, -, 3) &= \frac{1}{N_c} \mathbf{k}_1^2 \mathbf{k}_3^2 (K_{\text{BFKL}} \otimes D_2)(1, 3), \\ &= \frac{g^2}{2} [2c(13) - 2b(1, 3) - 2b(3, 1) + t(1, 3) + t(3, 1)]. \end{aligned} \quad (7)$$

This is becomes clear directly from the explicit form of the component functions to which we turn momentarily, and which also defines the convolution in this equation. Note that we understand the BFKL kernel to contain a delta function identifying the sums of the two incoming and the two outgoing momenta. Further, it can be proven that  $G$  vanishes when its first or last momentum argument vanishes,

$$G(1, 2, -) = G(-, 2, 3) = 0. \quad (8)$$

This is because then the component functions either vanish or turn into a different component function with fewer arguments (see below) and cancel among each other.

Let us now take a closer look at the component functions  $a$ ,  $b$ ,  $c$ ,  $s$  and  $t$ , of which  $G$  is composed. They were originally defined in momentum space [31] via

$$a(\mathbf{k}_1, \mathbf{k}_2, \mathbf{k}_3) = \int \frac{d^2 \mathbf{l}}{(2\pi)^3} \frac{\mathbf{k}_1^2}{(\mathbf{l} - \mathbf{k}_2)^2 (\mathbf{l} - \mathbf{k}_1 - \mathbf{k}_2)^2} D_2(\mathbf{l}, \mathbf{k}_1 + \mathbf{k}_2 + \mathbf{k}_3 - \mathbf{l}) \quad (9)$$

$$b(\mathbf{k}_1, \mathbf{k}_2) = \int \frac{d^2 \mathbf{l}}{(2\pi)^3} \frac{\mathbf{k}_1^2}{\mathbf{l}^2 (\mathbf{l} - \mathbf{k}_1)^2} D_2(\mathbf{l}, \mathbf{k}_1 + \mathbf{k}_2 - \mathbf{l}) \quad (10)$$

$$c(\mathbf{k}) = \int \frac{d^2 \mathbf{l}}{(2\pi)^3} \frac{\mathbf{k}^2}{\mathbf{l}^2 (\mathbf{l} - \mathbf{k})^2} D_2(\mathbf{l}, \mathbf{k} - \mathbf{l}) \quad (11)$$

$$s(\mathbf{k}_1, \mathbf{k}_2, \mathbf{k}_3) = \int \frac{d^2 \mathbf{l}}{(2\pi)^3} \frac{\mathbf{k}_1^2}{\mathbf{l}^2 (\mathbf{l} - \mathbf{k}_1)^2} D_2(\mathbf{k}_1 + \mathbf{k}_2, \mathbf{k}_3) \quad (12)$$

$$t(\mathbf{k}_1, \mathbf{k}_2) = \int \frac{d^2 \mathbf{l}}{(2\pi)^3} \frac{\mathbf{k}_1^2}{\mathbf{l}^2 (\mathbf{l} - \mathbf{k}_1)^2} D_2(\mathbf{k}_1, \mathbf{k}_2). \quad (13)$$

These functions are not infrared safe separately, but the infrared divergences cancel in the combination in which they occur in the function  $G$ .

There are some relations between the functions  $a$ ,  $b$  and  $c$  and between  $s$  and  $t$  and the so-called trajectory function  $\beta$ , namely

$$b(\mathbf{k}_1, \mathbf{k}_2) = a(\mathbf{k}_1, 0, \mathbf{k}_2) = a(\mathbf{k}_1, \mathbf{k}_2, 0) \quad (14)$$

$$c(\mathbf{k}) = b(\mathbf{k}, 0) = a(\mathbf{k}, 0, 0) \quad (15)$$

$$s(\mathbf{k}_1, \mathbf{k}_2, \mathbf{k}_3) = -\frac{2}{N_c g^2} \beta(\mathbf{k}_1) D_2(\mathbf{k}_1 + \mathbf{k}_2, \mathbf{k}_3) \quad (16)$$

$$t(\mathbf{k}_1, \mathbf{k}_2) = s(\mathbf{k}_1, 0, \mathbf{k}_2) = -\frac{2}{N_c g^2} \beta(\mathbf{k}_1) D_2(\mathbf{k}_1, \mathbf{k}_2) \quad (17)$$

The trajectory function  $\beta$  is defined in momentum space as

$$\beta(\mathbf{k}) = -\frac{N_c g^2}{2} \int \frac{d^2 \mathbf{l}}{(2\pi)^3} \frac{\mathbf{k}^2}{\mathbf{l}^2 (\mathbf{l} - \mathbf{k})^2}, \quad (18)$$

and the function  $\alpha(\mathbf{k}) = 1 + \beta(\mathbf{k})$  is known as the Regge trajectory of the gluon.

It is convenient to perform the calculation of the one-to-three Pomeron vertex in impact parameter space where one can make use of the properties of the function  $G$  and of the component functions under conformal transformations. These properties have first been studied in [30] where it was argued that  $G$  is invariant under conformal transformations in impact parameter space, i. e. under Möbius transformations of the coordinate arguments of  $G$ . This property was used in [34] to prove the conformal invariance of the two-to-six gluon vertex  $V_{2 \rightarrow 6}$ . For a more rigorous discussion of the conformal invariance of  $G$  and of the behaviour of the regularised component functions under conformal transformations see [35].

We therefore also need the impact parameter (or position space) representation of the component functions. The momentum space and positions space representations are related to each other via Fourier transformation, for the function  $G$  for example we have

$$G(\mathbf{k}_1, \mathbf{k}_2, \mathbf{k}_3) = \int \prod_{i=1}^3 \left[ d^2 \rho_i e^{-i \mathbf{k}_i \rho_i} \right] G(\rho_1, \rho_2, \rho_3). \quad (19)$$

In two-dimensional impact parameter space we use complex coordinates,  $\rho = \rho_x + i \rho_y$ . We use the same symbol for the momentum space representation and the position space



representation of a function, and again we often make use of the shorthand notation in which an index now stands for the corresponding coordinate. Let us now give the expressions for the component functions in complex coordinates [35]. For reasons to be explained in the next section we here use the notation  $D_2(\rho_1, \rho_2) = \Delta_1 \Delta_2 \Phi_2(\rho_1, \rho_2)$ . Then we have

$$a(\rho_1, \rho_2, \rho_3) = -\frac{1}{(2\pi)^3} \Delta_1 [\log 2 + \psi(1) - \log m - \log |\rho_{12}|] \cdot [\log 2 + \psi(1) - \log m - \log |\rho_{13}|] \Delta_2 \Delta_3 \Phi_2(\rho_2, \rho_3) \quad (20)$$

$$b(\rho_1, \rho_2) = \frac{1}{(2\pi)^2} \Delta_1 [\log 2 + \psi(1) - \log m - \log |\rho_{12}|] \Delta_2 \Phi_2(\rho_1, \rho_2) \quad (21)$$

$$c(\rho) = -\frac{1}{2\pi} \Delta \Phi_2(\rho, \rho) \quad (22)$$

$$s(\rho_1, \rho_2, \rho_3) = \frac{2}{(2\pi)^3} \left( 2\pi \delta^2(\rho_{12}) [\log 2 + \psi(1) - \log m - \log |\rho_{12}|] - \frac{1}{|\rho_{12}|^2} \right) \cdot \Delta_2 \Delta_3 \Phi_2(\rho_2, \rho_3) \quad (23)$$

$$t(\rho_1, \rho_2) = \frac{2}{(2\pi)^3} \int d^2 \rho_0 \left( 2\pi \delta^2(\rho_{10}) [\log 2 + \psi(1) - \log m - \log |\rho_{10}|] - \frac{1}{|\rho_{10}|^2} \right) \cdot \Delta_0 \Delta_2 \Phi_2(\rho_0, \rho_2), \quad (24)$$

where we have used the definition

$$\rho_{ij} = \rho_i - \rho_j. \quad (25)$$

These functions are regularised with a gluon mass  $m$ , and the limit  $m \rightarrow 0$  is implied in all expressions above. The expressions in square brackets are identical to the expansion of  $K_0$  Bessel functions for small arguments which originate from the configuration-space gluon propagator,

$$K_0(z) = \log 2 + \psi(1) - \log z + \mathcal{O}(z^2). \quad (26)$$

In the following, we will for brevity often choose to write  $K_0$  instead of the expansion.

In position space the relations between the five component functions and the trajectory function  $\beta$  have the following form:

$$b(\rho_1, \rho_2) = \int d^2 \rho' a(\rho_1, \rho', \rho_2) = \int d^2 \rho' a(\rho_1, \rho_2, \rho') \quad (27)$$

$$c(\rho) = \int d^2 \rho' b(\rho, \rho') = \int d^2 \rho' d^2 \rho'' a(\rho, \rho', \rho'') \quad (28)$$

$$s(\rho_1, \rho_2, \rho_3) = -\frac{2}{N_c g^2} \beta(\rho_{12}) \Delta_2 \Delta_3 \Phi_2(\rho_2, \rho_3) \quad (29)$$

$$t(\rho_1, \rho_2) = \int d^2 \rho_0 s(\rho_1, \rho_0, \rho_2) = -\frac{2}{N_c g^2} \int d^2 \rho_0 \beta(\rho_{10}) \Delta_0 \Delta_2 \Phi_2(\rho_0, \rho_2). \quad (30)$$

In addition we have the equivalent of the relation (7) in position space. Here the function  $G$  reduces to a double Laplacian of the well-known BFKL kernel multiplied by a constant when the second momentum argument is set to zero,

$$G(1, -, 3) = \frac{1}{N_c} \Delta_1 \Delta_3 (K_{\text{BFKL}} \otimes D_2)(1, 3). \quad (31)$$

Let us finally note that the representation (5) for the two-to-six vertex is easily generalised to other (even) numbers of reggeised gluons. In fact the  $2 \rightarrow 4$  reggeised gluon vertex can be written as a sum over functions ( $VD_2$ ) which are defined in terms of the function  $G$  in analogy to (5) [27]. In that case the sum runs over all (three) partitions of four indices into two groups of two. It is conjectured that there exist higher  $2 \rightarrow 2n$  reggeised gluon vertices which are also new elements of the effective field theory of unitarity corrections and which are of analogous form [34].

### 2.3 Multi-Pomeron vertices

We will now use the  $2 \rightarrow 2n$  reggeised gluon vertices of the EGLLA in order to define  $1 \rightarrow n$  Pomeron vertices. We will give the definition explicitly only for  $n = 2, 3$ , but assuming the existence of the higher  $2 \rightarrow 2n$  reggeised gluon vertices it is straightforward to extend the definition to arbitrary  $n$ . Due to the conformal invariance of the amplitudes of the EGLLA in impact parameter space it is most convenient to consider also the multi-Pomeron vertices in impact parameter space.

The vertices of the effective field theory for the  $n$ -gluon amplitudes in the EGLLA couple states with different numbers of reggeised gluons to each other. The vertex  $V_{2 \rightarrow 4}$  for example couples a two-gluon state to a general four-gluon state. By construction the two-gluon state is a BFKL Pomeron state which is coupled to a virtual photon impact factor. The vertex is separated in rapidity from that quark loop by Pomeron evolution. Due to high energy factorization the vertex is hence independent of the photon impact factor. In the following we will therefore use a pure BFKL Pomeron amplitude  $\Phi_2$  instead of the amplitude  $D_2$  containing the photon impact factor. More precisely, one usually choses to replace (removing two propagators)

$$D_2(\rho_1, \rho_2) \longrightarrow \Delta_1 \Delta_2 \Phi_2(\rho_1, \rho_2), \quad (32)$$

and we will follow this convention also for the  $1 \rightarrow 3$  Pomeron vertex further below. One then obtains the one-to-two Pomeron vertex from the  $2 \rightarrow 4$  reggeised gluon vertex  $V_{2 \rightarrow 4}$  by choosing the four-gluon state to be a product of two BFKL Pomeron states [27, 29]. In this way one projects two pairs of outgoing gluons onto BFKL Pomeron states.

Due to the conformal invariance of the BFKL kernel the BFKL Pomeron can be expanded in conformal partial waves [51]. It is therefore sufficient to consider the one-to-two Pomeron vertex for these conformal partial waves which are given by eigenfunctions of the BFKL kernel. The eigenfunctions are given by

$$E^{(\nu, n)}(\rho_1, \rho_2) = \left( \frac{\rho_{12}}{\rho_{1a}\rho_{2a}} \right)^h \left( \frac{\rho_{12}^*}{\rho_{1a}^*\rho_{2a}^*} \right)^{\bar{h}}. \quad (33)$$

According to the representation theory of the group  $SL(2, \mathbb{C})$  of conformal transformations in two dimensions the eigenfunctions are parametrised by the conformal weight

$$h = \frac{1+n}{2} + i\nu, \quad (34)$$

where  $n \in \mathbb{Z}$  is the integer conformal spin, and  $\nu$  takes on arbitrary real values. In (33) we have used  $\bar{h} = 1 - h^*$ . The eigenfunctions  $E(\nu, n)$  of the BFKL kernel depend

on an additional parameter,  $\rho_a$  in the case of eq. (33), which can be interpreted as the centre-of-mass coordinate of the Pomeron state. In the following the dependence on this additional parameter will always be understood but often not be written out explicitly. In the high energy limit the leading contribution to the BFKL Pomeron comes from the state with vanishing conformal spin  $n = 0$ , and only for this case the one-to-two Pomeron vertex has been calculated explicitly.

One defines the one-to-two Pomeron vertex as

$$V_{\mathbb{P} \rightarrow 2\mathbb{P}} = \delta_{a_1 a_2} \delta_{a_3 a_4} \left[ (V_{2 \rightarrow 4}^{a_1 a_2 a_3 a_4} D_2)(1, 2, 3, 4) \right]_{\Phi_2 // E^{(\nu_c, n_c)}} \otimes E^{(\nu_a, n_a)*}(1, 2) E^{(\nu_b, n_b)*}(3, 4). \quad (35)$$

The convolution  $\otimes$  is defined as an integral  $\int d\rho_1 \dots d\rho_4$  over the coordinates of all four outgoing gluons of the  $2 \rightarrow 4$  vertex. Due to the complete symmetry of the vertex  $V_{2 \rightarrow 4}$  in the four outgoing gluons it is not relevant which pairs of gluons are assumed to form Pomeron states. Here we have for simplicity chosen the pairs (1, 2) and (3, 4). The Pomerons are colour singlet states and the projection in colour space is performed via the contraction of the colour tensor of the vertex  $V_{2 \rightarrow 4}$  with delta-tensors for the pairs of gluons corresponding to the Pomeron states. Note that we have chosen the outgoing Pomerons to be represented by complex conjugated eigenfunctions. We implicitly assume that  $D_2$  is replaced by a pure BFKL amplitude according to (32). As indicated in the subscript of the square bracket we further replace the full amplitude  $\Phi_2$  by an eigenfunction  $E^{(\nu, n)}$  of the BFKL kernel. The resulting quantity contains all relevant information of the coupling of the three Pomerons with the parameters  $\{\rho_i, h_i\}$ , and the corresponding amplitude with three full Pomeron states is easily reconstructed. We will in the following always use the amplitude  $D_2$  in the sense that it has to be replaced according to (32), in particular also inside the function  $G$ .

The projection (35) has been performed explicitly in [29]. The resulting  $1 \rightarrow 2$  Pomeron vertex was found to be a conformal three-point function of the three Pomeron coordinates,

$$V_{\mathbb{P} \rightarrow 2\mathbb{P}} = C_{\{h_i, \bar{h}_i\}} \left[ \rho_{ab}^{h_a+h_b-h_c} \rho_{bc}^{h_b+h_c-h_a} \rho_{ac}^{h_a+h_c-h_b} \rho_{ab}^{*\bar{h}_a+\bar{h}_b-\bar{h}_c} \rho_{bc}^{*\bar{h}_b+\bar{h}_c-\bar{h}_a} \rho_{ac}^{*\bar{h}_a+\bar{h}_c-\bar{h}_b} \right]^{-1}, \quad (36)$$

where  $\rho_a$  is the coordinate of the Pomeron state with quantum numbers  $(\nu_a, n_a)$  etc., and the coefficient  $C_{\{h_i, \bar{h}_i\}}$  depends only on the conformal weights of the three Pomeron states. This finding motivates the symbolic notation of the vertex as a three-point correlation function,

$$V_{\mathbb{P} \rightarrow 2\mathbb{P}} = \left\langle E^{(\nu_a, n_a)*}(\rho_a) E^{(\nu_b, n_b)*}(\rho_b) E^{(\nu_c, n_c)}(\rho_c) \right\rangle. \quad (37)$$

The coefficient  $C_{\{h_i, \bar{h}_i\}}$  in the  $1 \rightarrow 2$  Pomeron vertex is the sum of two terms, one of which is suppressed by two powers of  $N_c$  with respect to the other. The numerical value of these two terms in the perturbative  $1 \rightarrow 2$  Pomeron vertex was found in [46] for the Pomeron ‘ground states’ with  $h = 1/2$  which are leading in the high energy limit. The value of the term leading in  $N_c$  obtained in this way starting from the ELLA coincides exactly with the value found in [47, 48] in the dipole picture of high energy scattering which is based on the large- $N_c$  limit. In [52] the value of the perturbative  $1 \rightarrow 2$  Pomeron vertex was later found to be of the same order of magnitude as nonperturbative

estimates of the triple-Pomeron vertex in Regge-type fits to scattering data at high energies.

The formula for the  $1 \rightarrow 2$  Pomeron vertex obtained in the dipole picture in [47, 48] exhibits a relatively simple structure. Motivated by this observation a generalisation of that formula to  $1 \rightarrow n$  Pomeron vertices with arbitrary  $n$  was conjectured in [50] motivated by results of [16]. Interestingly, this generalised formula could be related to dual Shapiro-Virasoro amplitudes of a closed string theory. However, in [30] it was shown that in the dipole picture a direct transition, i. e. a transition local in rapidity, from one to more than two Pomerons is not possible. Instead, in the framework of the dipole picture such a transition can only occur via the iteration of the  $1 \rightarrow 2$  Pomeron vertex, resulting in the well-known fan diagrams. The latter result does not necessarily exclude the existence of such vertices in general. Instead, it is well conceivable that it is the outcome of the large- $N_c$  limit used in the dipole picture. A natural next step beyond the limitations of the dipole model would be to include also higher multipoles. It is well conceivable that in such an extension of the dipole model (including quadrupoles for instance) a direct  $1 \rightarrow 3$  Pomeron vertex would occur and possibly be of the form suggested in [50].

The perturbative  $1 \rightarrow 3$  Pomeron vertex is defined in analogy to the  $1 \rightarrow 2$  Pomeron vertex above, now using the  $2 \rightarrow 6$  gluon vertex discussed in detail in the previous section. Due to the complete symmetry of that vertex in the six outgoing gluons it again does not matter which gluons are chosen to form Pomeron states. We choose the pairs  $(1, 2)$ ,  $(3, 4)$ , and  $(5, 6)$ , and the coordinates of these three Pomeron states will be  $\rho_a$ ,  $\rho_b$ , and  $\rho_c$ , respectively. The Pomeron state attached to the vertex from above will have the coordinate  $\rho_d$ . We will often not write down the external coordinates as arguments, which coordinate is which will be clear from the conformal dimensions  $\nu_a$ ,  $\nu_b$ ,  $\nu_c$ , and  $\nu_d$ .

Hence the projection of the  $2 \rightarrow 6$  gluon vertex defining the  $1 \rightarrow 3$  Pomeron vertex can be written as

$$V_{\mathbb{P} \rightarrow 3\mathbb{P}} = \delta_{a_1 a_2} \delta_{a_3 a_4} \delta_{a_5 a_6} \left[ (V_{2 \rightarrow 6}^{a_1 a_2 a_3 a_4 a_5 a_6} D_2)(1, 2, 3, 4, 5, 6) \right]_{\Phi_2 // E^{(\nu_d, n_d)}} \otimes \\ \otimes E^{(\nu_a, n_a)*}(1, 2) E^{(\nu_b, n_b)*}(3, 4) E^{(\nu_c, n_c)*}(5, 6). \quad (38)$$

Note again our convention in which the three outgoing Pomerons are described by complex conjugated eigenfunctions. Anticipating that the vertex will turn out to have the form of a conformal four-point function we will also use the symbolic notation of the vertex as a correlation function

$$V_{\mathbb{P} \rightarrow 3\mathbb{P}} = \left\langle E^{(\nu_a, n_a)*}(\rho_a) E^{(\nu_b, n_b)*}(\rho_b) E^{(\nu_c, n_c)*}(\rho_c) E^{(\nu_d, n_d)}(\rho_d) \right\rangle. \quad (39)$$

In the present paper we will restrict ourselves to the leading Pomeron states at high energies, i. e. the states with  $n_i = 0$ , and this applies to all four Pomeron states in the  $1 \rightarrow 3$  Pomeron vertex.

The Pomeron vertices defined above are constructed from the number-changing vertices  $V_{2 \rightarrow 4}$  and  $V_{2 \rightarrow 6}$  of the ELLA. It should be pointed out, however, that also other terms in the  $n$ -gluon amplitudes  $D_n$  can in general give rise to multi-Pomeron vertices. In the case of the  $1 \rightarrow 2$  Pomeron vertex for example also the reggeising part of the amplitude, i. e. the first term in (2), gives a nonvanishing contribution upon

projection on Pomeron states. So far this contribution has not yet been studied in much detail. In the case of the six-gluon amplitude  $D_6$  there are two such reggeising terms, one being a superposition of two-gluon amplitudes and the other being a superposition of irreducible four-gluon amplitudes. We will not consider the contribution of these terms to the  $1 \rightarrow 3$  Pomeron vertex in the present paper. These terms can well be important and clearly deserve further study. First steps in this direction have been performed in [35].

### 3 The $1 \rightarrow 3$ Pomeron vertex

#### 3.1 The colour structure

The two gluons in a Pomeron form a colour singlet state, and hence the corresponding colour structure is  $\delta_{ab}$ . Because the symmetric structure constants  $d_{abc}$  vanish when two of their indices are contracted less than half of the terms in the sum in (4) contribute to the  $1 \rightarrow 3$  Pomeron vertex. The only remaining terms are those in which the two colour indices of each Pomeron are contracted with different  $d$  tensors. Since we chose as Pomerons the pairs (12), (34) and (56) of gluons, this leaves the following four permutations of (colour, momentum or coordinate) indices:

$$(1, 3, 5; 2, 4, 6), \quad (1, 3, 6; 2, 4, 5), \quad (1, 4, 5; 2, 3, 6), \quad \text{and} \quad (1, 4, 6; 2, 3, 5). \quad (40)$$

Each of these permutations gives rise to the same colour factor because of the symmetry of  $d_{abc}$ . Since each  $d_{abc}$  tensor is contracted with one index of each of the  $\delta$ s, the result is the contraction of two  $d$  tensors. For general  $N_c$  we denote this contraction by  $C$ . Its value is, calculated for example for the first permutation,

$$C = d_{a_1 a_3 a_5} d_{a_2 a_4 a_6} \delta_{a_1 a_2} \delta_{a_3 a_4} \delta_{a_5 a_6} = d_{a_1 a_3 a_5} d_{a_1 a_3 a_5} = \frac{1}{N_c} (N_c^2 - 4)(N_c^2 - 1). \quad (41)$$

#### 3.2 The spatial part

##### 3.2.1 Introduction

The lion's share of the work to be done for the projection is sorting out all the terms of the spatial part of  $V_{2 \rightarrow 6}$ . This work is complicated by the fact that the simple representation of  $V_{2 \rightarrow 6}$  in terms of  $G$  does not help in obtaining the  $1 \rightarrow 3$  Pomeron vertex. That is because due to  $E^{(\nu,0)}(\rho, \rho) = 0$  some of the component functions of  $G$  vanish on projection, others don't.

The brute-force way of extracting those that remain would be to write out  $(WD_2)$  in terms of the functions  $a, b, c, s$  and  $t$  and sort out those that vanish upon projection. However, there is a more systematic way. First, we observe that the four permutations (40) remaining after the contraction of colour tensors all lead to the same term. This is because they differ only by swapping two coordinates of the same Pomeron wave function, which is symmetric. Hence it is sufficient to consider only one of the permutations and multiply the result by four.

The second important observation is that the conformal eigenfunctions  $E^{(\nu,0)}$  vanish if their two coordinate arguments are equal,  $E^{(\nu,0)}(\rho, \rho) = 0$ . Therefore terms in which both argument indices of the same Pomeron occur in the same argument of  $G$  vanish

under projection. This is the key to finding out which terms remain after projection. Let us now have a look at the first permutation in (40). The spatial part of the vertex for this permutation has the following form:

$$(WD_2)(1, 3, 5; 2, 4, 6) = \frac{g^4}{8} \sum_{M \in \mathcal{P}(\{1, \dots, 6\})} (-1)^{\#M} G(135 \setminus M, M, 246 \setminus M). \quad (42)$$

We can see immediately that a term from this sum vanishes if two coordinates of the same Pomeron are contained in the middle argument of  $G$ . The first and last argument of  $G$  contain only coordinates or momenta belonging to different Pomerons and hence cannot cause the term to vanish under projection. Therefore all the terms for which  $M$  does not contain both indices of a Pomeron remain:

$$(WD_2)_{\mathbb{P} \rightarrow 3\mathbb{P}}(1, 3, 5; 2, 4, 6) = \frac{g^4}{8} \sum_{\substack{M \in \mathcal{P}(\{1, \dots, 6\}) \\ M \not\supset \{1, 2\} \wedge M \not\supset \{3, 4\} \wedge M \not\supset \{5, 6\}}} (-1)^{\#M} G(135 \setminus M, M, 246 \setminus M). \quad (43)$$

In words:  $M$  may contain either 1 or 2 or none of these two indices, and 3 or 4 or neither of them, and 5 or 6 or neither. This yields  $3 \cdot 3 \cdot 3 = 27$  terms. However, two of these vanish because of a property of the  $G$  function: It vanishes when its first or third argument is empty, see Eq. (8). This eliminates the terms for  $M = \{1, 3, 5\}$  and  $M = \{2, 4, 6\}$ . Hence 25 terms remain.

The function  $G$  is composed of functions with one, two and with three arguments. The function with one argument,  $c$ , does not contribute at all to the Pomeron vertex. Since its argument always contains all indices,  $c$  does not survive the projection. The functions with two arguments,  $b$  and  $t$ , are also components of the BFKL kernel. We will discuss them in the next part of this section. The functions with three arguments,  $a$  and  $s$ , will be dealt with after that.

### 3.2.2 The BFKL term

The functions  $b$  and  $t$  survive only if they are convoluted with Pomerons in one specific way, namely if each Pomeron's arguments are convoluted with different arguments of  $b$  or  $t$ . This means that both arguments of  $b$  resp.  $t$  contain three indices, one from each Pomeron. First of all, this is the case for the term in (5) where  $M = \emptyset$ .

Besides, there are terms in the sum (43) where  $M$  contains only indices from the first or only from the second group of arguments of  $(WD_2)$ . Since one argument of  $b$  and  $t$  contains two arguments of  $G$  taken together (see (6)), one of the two  $b$  and  $t$  functions would have momenta of different Pomerons in each argument and hence would contribute. However, by replacing  $M$  by its complement with respect to the group of arguments of  $(WD_2)$ , an identical term with opposite sign can be obtained (unless  $M$  is identical to the whole group of arguments, but these terms vanish, see above). Therefore all such terms cancel out.

To illustrate this, let us look at an example. We again consider the first of the permutations in (40) with the spatial function (42). For example,  $M = \{1, 3\}$  contains only indices from the first three arguments of  $(WD_2)$ . The corresponding term in the sum contains the following  $G$  function:

$$G(5, 13, 246) = \frac{g^2}{2} [2c(123456) - 2b(135, 246) - 2b(12346, 5) + 2a(13, 5, 246) + t(135, 246) + t(12346, 5) - s(13, 5, 246) - s(13, 246, 5)] . \quad (44)$$

The terms with more than three indices in one argument, such as  $c$  and the second  $b$  and  $t$  functions, vanish because this identifies two coordinates of a Pomeron. For now, we ignore the functions  $a$  and  $s$ ; we will deal with them in the next section. The remaining terms,  $-2b(135, 246)$  and  $t(135, 246)$  do not vanish. However, the same terms occur in the term for the complement of  $M$ ,  $M' = \{1, 3, 5\} \setminus M = \{5\}$ . The corresponding  $G$  function is:

$$G(13, 5, 246) = \frac{g^2}{2} [2c(123456) - 2b(135, 246) - 2b(2456, 13) + 2a(5, 13, 246) + t(135, 246) + t(2456, 13) - s(5, 13, 246) - s(5, 246, 13)] . \quad (45)$$

Again,  $-2b(135, 246)$  and  $t(135, 246)$  remain. But this term has the opposite sign because of the prefactor  $(-1)^{\#M}$ . So the  $t$  and  $b$  functions for  $M \neq \emptyset$  cancel out.<sup>2</sup>

Only for  $M = \emptyset$  the functions  $b$  and  $t$  contribute to the  $1 \rightarrow 3$  Pomeron vertex. Knowing that  $G$  becomes a derivative of the BFKL kernel when its middle momentum argument vanishes (see Eq. (31)), we can immediately write out this term. Since there is one such term for each of the four permutations whose colour structure does not vanish, we have to multiply the result by 4. We now replace the full amplitude  $\Phi_2$  in  $G$  by the eigenfunction  $E^{(\nu_d, 0)}$  of the BFKL kernel as discussed in section 2.3 and obtain the following BFKL term:

$$\begin{aligned} V_{\mathbb{P} \rightarrow 3\mathbb{P}}^{BFKL} &= C \frac{g^4}{8} 4 \int d^2 \rho_1 d^2 \rho_2 E^{(\nu_a, 0)*}(\rho_1, \rho_2) E^{(\nu_b, 0)*}(\rho_1, \rho_2) E^{(\nu_c, 0)*}(\rho_1, \rho_2) \cdot \\ &\quad \cdot \frac{1}{N_c} \Delta_1 \Delta_2 (K_{BFKL} \otimes E^{(\nu_d, 0)})(\rho_1, \rho_2) \\ &= C \frac{g^4}{8} 4 \frac{\chi(\nu_d, 0)}{N_c} \int \frac{d^2 \rho_1 d^2 \rho_2}{|\rho_{12}|^4} E^{(\nu_a, 0)*}(\rho_1, \rho_2) E^{(\nu_b, 0)*}(\rho_1, \rho_2) \cdot \\ &\quad \cdot E^{(\nu_c, 0)*}(\rho_1, \rho_2) E^{(\nu_d, 0)}(\rho_1, \rho_2) \\ &= C \frac{g^6}{16} 4 \frac{2}{(2\pi)^3} \xi(\nu_d) (4\nu_d^2 + 1)^2 \int \frac{d^2 \rho_1 d^2 \rho_2}{|\rho_{12}|^4} \left( \frac{|\rho_{12}|}{|\rho_{1a}||\rho_{2a}|} \right)^{1-2i\nu_a} \cdot \\ &\quad \cdot \left( \frac{|\rho_{12}|}{|\rho_{1b}||\rho_{2b}|} \right)^{1-2i\nu_b} \left( \frac{|\rho_{12}|}{|\rho_{1c}||\rho_{2c}|} \right)^{1-2i\nu_c} \left( \frac{|\rho_{12}|}{|\rho_{1d}||\rho_{2d}|} \right)^{1+2i\nu_d} . \end{aligned} \quad (46)$$

We have evaluated the convolution with the BFKL kernel using the BFKL eigenvalue

$$\int d^2 \rho'_1 d^2 \rho'_2 K_{BFKL}(\rho_1, \rho_2; \rho'_1, \rho'_2) E^{(\nu, n)}(\rho'_1, \rho'_2) = \chi(\nu, n) E^{(\nu, n)}(\rho_1, \rho_2) , \quad (47)$$

and put in the derivative of the wave function (93). In addition, in the last step we have rewritten the BFKL eigenvalue  $\chi$  as a function  $\xi$  which was already used in [29]. It

---

<sup>2</sup>The deeper reason for this is that  $6/2 = 3$  is odd. It can be conjectured that the same mechanism of cancellation occurs in the projection of higher  $1 \rightarrow n$  Pomeron vertices from  $2 \rightarrow 2n$  reggeised gluon vertices for odd  $n$ .

differs from  $\chi$  only in that it does not contain factors of  $N_c$  and the coupling constant:

$$\xi(\nu) = 2\pi \left[ 2\psi(1) - \psi\left(\frac{1}{2} + i\nu\right) - \psi\left(\frac{1}{2} - i\nu\right) \right] = \frac{8\pi^3}{N_c g^2} \chi(\nu, 0). \quad (48)$$

Figure 1 shows a graphical representation of this part of the vertex.



Figure 1: Graphical representation of the part of the  $1 \rightarrow 3$  Pomeron vertex which contains the BFKL kernel. The half-circular lines indicate Pomeron wave functions.

### 3.2.3 The $\alpha$ terms

What remains now are the functions with three arguments,  $a$  and  $s$ . Since they have the same properties (both vanish only when their first argument, i. e. the second argument of  $G$ , is empty), they always occur together, and the result of the projection can be expressed in terms of the function  $\alpha$  defined as

$$\alpha(2, 1, 3) = 2a(2, 1, 3) - s(2, 1, 3) - s(2, 3, 1). \quad (49)$$

$\alpha$  is symmetric in its last two arguments. Figure 2 shows a graphical representation of this equation using the diagrammatic notation used for example in [31]. The middle leg of  $\alpha$ , which corresponds to its first argument, is marked to remind us of the fact that  $\alpha$  is symmetric in the other two arguments, but not this one.

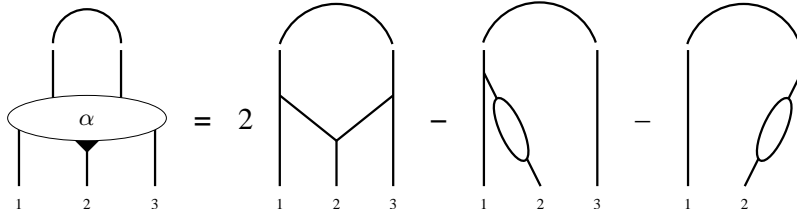


Figure 2: Graphical representation of Eq. (49). The arcs represent Pomeron wave functions defined into the functions  $a$ ,  $s$  and  $\alpha$ .

We will now divide the remaining terms from (43) into groups that lead to the same type of integral after convolution with the wave functions. There are 24 terms since the case  $M = \emptyset$  has already been dealt with above. The most obvious classification criterion is the number of elements  $M$  contains, i. e. the number of momenta or coordinates in the first argument of  $\alpha$ . There are six terms for which  $M$  has one element,



twelve for which it has two and six with three elements. (Normally there would be eight in the last class, but for two of them  $M$  contains a whole group of arguments and  $G$  vanishes, see above.) Not that it is quite natural that the numbers of terms in all classes are divisible by six. Six is the number of permutations of three objects. Because of the high symmetry of the  $2 \rightarrow 6$  reggeised gluon vertex, there are terms with every Pomeron coupling to every pair of arguments of the function  $G$ . Terms which differ only by permutations of the labels (= external coordinates) of the Pomerons belong to the same class since they lead to the same type of integral. The terms from different classes contribute with different signs due to the factor  $(-1)^{\#M}$  in (42). The second class has positive sign, the others negative sign.

The second of the classes presented above can be subdivided further. It contains those terms for which  $M$ , and hence the first argument of  $\alpha$ , contains two indices. It makes a difference whether the second and third arguments also contain two or whether one has three and the other only one. With this subdivision, we have four classes in total, with six terms each. There is an intuitive interpretation of these classes which is presented graphically in Figure 3. The classes differ in how many Pomerons are attached to the different legs of the  $\alpha$  function.

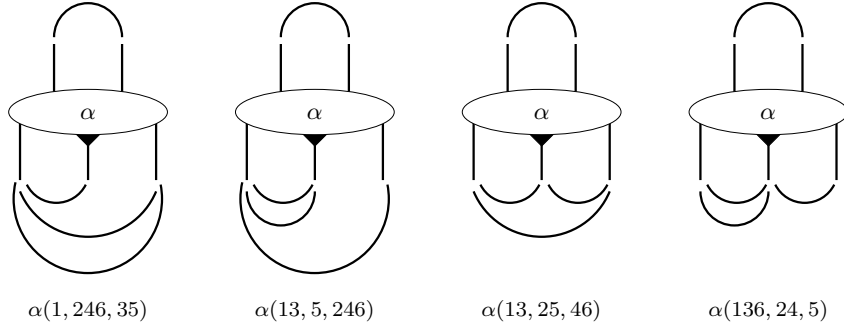


Figure 3: Graphical representation of the classes of terms with the  $\alpha$  function. One representative term is printed underneath each graph (assuming the Pomerons (12), (34) and (56)). The half-circular lines indicate Pomeron wave functions.

Bearing in mind that  $\alpha$  is symmetric in its last two arguments but not its first, it is easy to see that the four classes are indeed disjoint. What is more, they are also complete. It is impossible to construct a term which does not belong to one of the classes (taking into account the properties of  $\alpha$  and the Pomeron amplitude).

### 3.2.4 A closer look at the $\alpha$ terms

Before writing down the integrals containing  $\alpha$  which make up the largest part of the  $1 \rightarrow 3$  Pomeron vertex, let us write down the configuration space form of  $\alpha$ :

$$\begin{aligned} \alpha(\rho_2, \rho_1, \rho_3) &= \frac{2}{(2\pi)^3} \left[ -\Delta_2 K_0(m|\rho_{12}|) K_0(m|\rho_{23}|) - \left( 2\pi \delta^2(\rho_{12}) K_0(m|\rho_{12}|) - \frac{1}{|\rho_{12}|^2} \right) \right. \\ &\quad \left. - \left( 2\pi \delta^2(\rho_{23}) K_0(m|\rho_{23}|) - \frac{1}{|\rho_{23}|^2} \right) \right] \Delta_1 \Delta_3 \Phi_2(\rho_1, \rho_3) \\ &= \frac{2}{(2\pi)^3} \left[ - \left( -2\pi \delta^2(\rho_{12}) K_0(m|\rho_{23}|) + \frac{1}{\rho_{12}^* \rho_{23}^*} + \frac{1}{\rho_{12}^* \rho_{23}} \right) \right] \end{aligned}$$

$$\begin{aligned}
& - 2\pi \delta^2(\rho_{23}) K_0(m|\rho_{12}|) \Big) - 2\pi \delta^2(\rho_{12}) K_0(m|\rho_{12}|) \\
& - 2\pi \delta^2(\rho_{23}) K_0(m|\rho_{23}|) + \frac{1}{|\rho_{12}|^2} + \frac{1}{|\rho_{23}|^2} \Big] \Delta_1 \Delta_3 \Phi_2(\rho_1, \rho_3) \\
& = \frac{2}{(2\pi)^3} \left[ - 2\pi(\delta^2(\rho_{12}) - \delta^2(\rho_{23}))(K_0(m|\rho_{12}|) - K_0(m|\rho_{23}|)) \right. \\
& \quad \left. + \left| \frac{1}{\rho_{12}} + \frac{1}{\rho_{23}} \right|^2 \right] \Delta_1 \Delta_3 \Phi_2(\rho_1, \rho_3) \\
& = \frac{2}{(2\pi)^3} \left[ 2\pi(\delta^2(\rho_{12}) - \delta^2(\rho_{23})) \log \frac{|\rho_{12}|}{|\rho_{23}|} + \left| \frac{\rho_{13}}{\rho_{12}\rho_{23}} \right|^2 \right] \Delta_1 \Delta_3 \Phi_2(\rho_1, \rho_3), \quad (50)
\end{aligned}$$

where we have made use of the identity  $\partial(1/\rho^*) = \partial^*(1/\rho) = \pi\delta^2(\rho)$ .

The two delta functions identify the second or third coordinate argument of  $G$  with its first. When this function is convoluted with further Pomeron wave functions as illustrated in Figure 3, one or both of the delta function terms vanish after integration because the delta functions identify two coordinates of a Pomeron. For the last two groups in that Figure both delta function terms vanish (since there are Pomerons between the middle and both outer legs of  $\alpha$ ), for the others only one.

Several terms of the function  $\alpha$  are potentially divergent under an integral. The terms  $\delta^2(\rho_{12}) \log |\rho_{12}|$  are obviously dangerous, but also the fraction may cause a logarithmic divergence with respect to the integration over  $\rho_{12}$  or  $\rho_{23}$ . The Pomeron wave function for zero conformal spin  $E^{(\nu,0)}(\rho_1, \rho_2)$  contains one power of  $|\rho_{12}|$  and can hence regularise these divergences. Eliminating the delta functions requires that a Pomeron is attached between the middle and one of the outer legs of  $\alpha$ . Therefore the terms from the last two groups in Figure 3 are finite while in the others one divergence remains and has to be regularised.

We will now write down the integrals resulting from each of the four groups of terms. We will denote them (and the groups) with an upper index equal to  $\#M$ , the number of elements in  $M$ . The two groups with  $\#M = 2$  will be distinguished by the minimal number of coordinates in the other arguments of the  $G$  function and denoted by “(2,1)” and “(2,2)”.

The trajectory function contains two terms which are ultraviolet divergent under an integral and have to be regularised:  $1/|\rho|^2$  and  $\delta(\rho) \log \rho$ . We regularise the fraction  $1/|\rho|^2$  with a theta function  $\theta(|\rho| - \epsilon)$ , i.e. a UV cutoff. The term  $\delta^2(\rho) \log |\rho|$  is regularised by replacing  $\log |\rho|$  with  $\log \epsilon$ .

For the first group of terms ( $\#M = 1$ ), we obtain

$$\begin{aligned}
V_{\mathbb{P} \rightarrow 3\mathbb{P}}^{(1)} & = -C \frac{g^6}{16} 4 \sum_{a \leftrightarrow b \leftrightarrow c} \int d^2 \rho_1 d^2 \rho_2 d^2 \rho_3 d^2 \rho_4 d^2 \rho_5 d^2 \rho_6 E^{(\nu_a,0)*}(\rho_1, \rho_2) E^{(\nu_b,0)*}(\rho_3, \rho_4) \cdot \\
& \cdot E^{(\nu_c,0)*}(\rho_5, \rho_6) \delta^2(\rho_{24}) \delta^2(\rho_{26}) \delta^2(\rho_{35}) \frac{2}{(2\pi)^3} \left[ 2\pi \delta^2(\rho_{13}) \log \frac{\epsilon}{|\rho_{12}|} \right. \\
& \left. + \frac{|\rho_{23}|^2}{|\rho_{12}|^2 |\rho_{13}|^2} \theta(|\rho_{13}| - \epsilon) \right] \Delta_2 \Delta_3 E^{(\nu_d,0)}(\rho_2, \rho_3)
\end{aligned}$$

$$\begin{aligned}
&= -C \frac{g^6}{16} 4 \frac{2}{(2\pi)^3} \sum_{a \leftrightarrow b \leftrightarrow c} \int d^2 \rho_1 d^2 \rho_2 d^2 \rho_3 E^{(\nu_a, 0)*}(\rho_1, \rho_2) E^{(\nu_b, 0)*}(\rho_2, \rho_3) \cdot \\
&\quad \cdot E^{(\nu_c, 0)*}(\rho_2, \rho_3) \left[ 2\pi \delta^2(\rho_{13}) \log \frac{\epsilon}{|\rho_{12}|} + \frac{|\rho_{23}|^2}{|\rho_{12}|^2 |\rho_{13}|^2} \theta(|\rho_{13}| - \epsilon) \right] \cdot \\
&\quad \cdot \Delta_2 \Delta_3 E^{(\nu_d, 0)}(\rho_2, \rho_3). \tag{51}
\end{aligned}$$

The constant  $C$  is the colour factor, the factor 4 the combinatorial factor from the four permutations (40). The factor  $g^6/16$  is the product of the prefactors in  $(WD_2)$  and  $G$ . We have rewritten the sum over the six terms of this group as a sum over the permutations of the Pomeron indices which is equivalent to it by way of renaming the integration variables. It is denoted by  $\sum_{a \leftrightarrow b \leftrightarrow c}$ . We can now insert the explicit form of the Pomeron wave functions. This allows us to evaluate the double Laplacian calculated in the Appendix (see Eq. (93)), and we find

$$\begin{aligned}
V_{\mathbb{P} \rightarrow 3\mathbb{P}}^{(1)} &= \dots = -C \frac{g^6}{16} 4 \frac{2}{(2\pi)^3} (4\nu_d^2 + 1)^2 \sum_{a \leftrightarrow b \leftrightarrow c} \int d^2 \rho_1 d^2 \rho_2 d^2 \rho_3 \cdot \\
&\quad \cdot \left( \frac{|\rho_{12}|}{|\rho_{1a}||\rho_{2a}|} \right)^{1-2i\nu_a} \left( \frac{|\rho_{23}|}{|\rho_{2b}||\rho_{3b}|} \right)^{1-2i\nu_b} \left( \frac{|\rho_{23}|}{|\rho_{2c}||\rho_{3c}|} \right)^{1-2i\nu_c} \cdot \\
&\quad \cdot \left[ 2\pi \delta^2(\rho_{13}) \log \frac{\epsilon}{|\rho_{12}|} + \frac{|\rho_{23}|^2}{|\rho_{12}|^2 |\rho_{13}|^2} \theta(|\rho_{13}| - \epsilon) \right] \frac{1}{|\rho_{23}|^4} \left( \frac{|\rho_{23}|}{|\rho_{2d}||\rho_{3d}|} \right)^{1+2i\nu_d} \\
&= -C \frac{g^6}{16} 4 \frac{2}{(2\pi)^3} (4\nu_d^2 + 1)^2 \sum_{a \leftrightarrow b \leftrightarrow c} \int \frac{d^2 \rho_2 d^2 \rho_3}{|\rho_{23}|^4} \left( \frac{|\rho_{23}|}{|\rho_{2b}||\rho_{3b}|} \right)^{1-2i\nu_b} \cdot \\
&\quad \cdot \left( \frac{|\rho_{23}|}{|\rho_{2c}||\rho_{3c}|} \right)^{1-2i\nu_c} \left( \frac{|\rho_{23}|}{|\rho_{2d}||\rho_{3d}|} \right)^{1+2i\nu_d} \int d^2 \rho_1 \left[ 2\pi \delta^2(\rho_{13}) \log \epsilon \right. \\
&\quad \left. + \frac{|\rho_{23}|^2}{|\rho_{12}|^2 |\rho_{13}|^2} \theta\left(\frac{|\rho_{13}|}{|\rho_{12}|} - \epsilon\right) \right] \left( \frac{|\rho_{12}|}{|\rho_{1a}||\rho_{2a}|} \right)^{1-2i\nu_a} \tag{52}
\end{aligned}$$

We have converted a logarithm into a factor inside the theta function. This has the advantage that now the theta function is invariant under dilatations. It is done according to the following identity:

$$\begin{aligned}
&\lim_{\epsilon \rightarrow 0} \int d^2 \rho_1 \left( \frac{\theta(|\rho_{13}| - \epsilon/\lambda)}{|\rho_{13}|^2} f(\rho_1) - \frac{\theta(|\rho_{13}| - \epsilon)}{|\rho_{13}|^2} f(\rho_1) \right) = \\
&= \lim_{\epsilon \rightarrow 0} \int d^2 \rho_1 \frac{\theta(|\rho_{13}| - \epsilon/\lambda) - \theta(|\rho_{13}| - \epsilon)}{|\rho_{13}|^2} (f(\rho_3) + \mathcal{O}(\epsilon)) \\
&= 2\pi f(\rho_3) \lim_{\epsilon \rightarrow 0} \int_{\epsilon/\lambda}^{\epsilon} d|\rho_{13}| \frac{1}{|\rho_{13}|} \\
&= 2\pi \log \lambda f(\rho_3) \\
&= 2\pi \log \lambda \int d^2 \rho_1 \delta^2(\rho_{13}) f(\rho_1). \tag{53}
\end{aligned}$$

Here we have used it for  $\lambda = 1/|\rho_{12}|$  and  $f(\rho_1) = E^{(\nu_a, 0)*}(\rho_1, \rho_2)$ . One can argue [35] that (53) can be applied even when the factor  $\lambda$  contains the integration variable.

It is easily shown that  $V_{\mathbb{P} \rightarrow 3\mathbb{P}}^{(1)}$  alone has the transformation properties of a conformal four-point function. Invariance under translations and rotations is trivial. Invariance of the integral operator under dilatation with a factor  $\lambda$  is not hard to prove: The three integrals give a factor  $\lambda^6$ , the denominator  $|\rho_{23}|^4$  a factor  $\lambda^{-4}$ . Both the delta function and the fraction in the rectangular brackets give a factor  $\lambda^{-2}$ .

There remains inversion. The first two integrals together with the denominator are invariant. So is the  $\rho_1$  integral together with the delta function and the fraction. However, the theta function gives rise to an extra logarithmic term inside the brackets. Using relation (53) with respect to the  $\rho_1$  integration for  $\lambda = |\rho_2/\rho_3|$ , it is computed to  $|\rho_{23}|^2/|\rho_{12}|^2 \cdot 2\pi \delta(\rho_{13}) \log |\rho_2/\rho_3|$ . After performing the  $\rho_1$  integration, everything except this logarithm is symmetric under the exchange  $\rho_2 \leftrightarrow \rho_3$ . Hence the additional term is overall antisymmetric and vanishes under the integration over  $\rho_2$  and  $\rho_3$ .

The integrals resulting from the other groups of terms are derived analogously. In all cases, the remaining integration variables are  $\rho_1, \rho_2$  and  $\rho_4$ , which we will rename  $\rho_3$ . The second group, for which  $\#M = 2$  and one of the arguments of  $G$  contains only one coordinate, also requires regularisation. We deal with that as shown for  $V_{\mathbb{P} \rightarrow 3\mathbb{P}}^{(1)}$ , including absorbing the logarithm into the theta function. Like  $V_{\mathbb{P} \rightarrow 3\mathbb{P}}^{(1)}$ , the vertices belonging to the other groups are also conformal four-point functions on their own. Here they are:

$$\begin{aligned} V_{\mathbb{P} \rightarrow 3\mathbb{P}}^{(2,1)} = & C \frac{g^6}{16} 4 \frac{2}{(2\pi)^3} (4\nu_d^2 + 1)^2 \sum_{a \leftrightarrow b \leftrightarrow c} \int d^2 \rho_1 d^2 \rho_2 d^2 \rho_3 \frac{1}{|\rho_{12}|^4} \left( \frac{|\rho_{12}|}{|\rho_{1a}||\rho_{2a}|} \right)^{1-2i\nu_a} \cdot \\ & \cdot \left( \frac{|\rho_{13}|}{|\rho_{1b}||\rho_{3b}|} \right)^{1-2i\nu_b} \left( \frac{|\rho_{13}|}{|\rho_{1c}||\rho_{3c}|} \right)^{1-2i\nu_c} \left[ 2\pi \delta^2(\rho_{23}) \log \epsilon \right. \\ & \left. + \frac{|\rho_{12}|^2}{|\rho_{13}|^2 |\rho_{23}|^2} \theta \left( \frac{|\rho_{23}|}{|\rho_{13}|} - \epsilon \right) \right] \left( \frac{|\rho_{12}|}{|\rho_{1d}||\rho_{2d}|} \right)^{1+2i\nu_d} \end{aligned} \quad (54)$$

$$\begin{aligned} V_{\mathbb{P} \rightarrow 3\mathbb{P}}^{(2,2)} = & C \frac{g^6}{16} 4 \frac{2}{(2\pi)^3} (4\nu_d^2 + 1)^2 \sum_{a \leftrightarrow b \leftrightarrow c} \int d^2 \rho_1 d^2 \rho_2 d^2 \rho_3 \frac{1}{|\rho_{12}|^2 |\rho_{13}|^2 |\rho_{23}|^2} \cdot \\ & \cdot \left( \frac{|\rho_{12}|}{|\rho_{1a}||\rho_{2a}|} \right)^{1-2i\nu_a} \left( \frac{|\rho_{13}|}{|\rho_{1b}||\rho_{3b}|} \right)^{1-2i\nu_b} \left( \frac{|\rho_{23}|}{|\rho_{2c}||\rho_{3c}|} \right)^{1-2i\nu_c} \left( \frac{|\rho_{23}|}{|\rho_{2d}||\rho_{3d}|} \right)^{1+2i\nu_d} \end{aligned} \quad (55)$$

$$\begin{aligned} V_{\mathbb{P} \rightarrow 3\mathbb{P}}^{(3)} = & -C \frac{g^6}{16} 4 \frac{2}{(2\pi)^3} (4\nu_d^2 + 1)^2 \sum_{a \leftrightarrow b \leftrightarrow c} \int d^2 \rho_1 d^2 \rho_2 d^2 \rho_3 \frac{1}{|\rho_{12}|^2 |\rho_{13}|^2 |\rho_{23}|^2} \cdot \\ & \cdot \left( \frac{|\rho_{12}|}{|\rho_{1a}||\rho_{2a}|} \right)^{1-2i\nu_a} \left( \frac{|\rho_{13}|}{|\rho_{1b}||\rho_{3b}|} \right)^{1-2i\nu_b} \left( \frac{|\rho_{13}|}{|\rho_{1c}||\rho_{3c}|} \right)^{1-2i\nu_c} \left( \frac{|\rho_{23}|}{|\rho_{2d}||\rho_{3d}|} \right)^{1+2i\nu_d} \end{aligned} \quad (56)$$

### 3.3 Simplifying the spatial part and the function $\Psi$

#### 3.3.1 The $1 \rightarrow 3$ Pomeron vertex as a conformal four-point function

In the previous section we have learnt that each of the five terms of the  $1 \rightarrow 3$  Pomeron vertex is a conformal four-point function. This means that they are severely constrained in their form. The general form can be simplified even further because we use only ground state wave functions for the Pomerons, so that the two conformal weights are equal:  $h = \bar{h} = \frac{1}{2} + i\nu$ . Besides, we have to take into account that we have used complex conjugated wave functions for the Pomerons attached to the vertex from below. This is equivalent to replacing  $\nu \rightarrow -\nu$ . The resulting formula for our four-point function reads:

$$\begin{aligned} \left\langle E^{(\nu_a,0)*}(\rho_a) E^{(\nu_b,0)*}(\rho_b) E^{(\nu_c,0)*}(\rho_c) E^{(\nu_d,0)}(\rho_d) \right\rangle = \\ = \Psi(x, x^*; \{\nu_i\}) \prod_{i < j} |\rho_{ij}|^{2i(-\tilde{\nu}_i - \tilde{\nu}_j + \frac{1}{3} \sum_k \tilde{\nu}_k)}, \end{aligned} \quad (57)$$

$$x = \frac{\rho_{ab}\rho_{cd}}{\rho_{ac}\rho_{bd}}, \quad (58)$$

where  $\tilde{\nu}_i$  is  $-\nu_i$  for  $i = a, b, c$  and  $\nu_d$  for  $i = d$ . The sum over  $k$  in the exponent runs over the four indices  $a, \dots, d$ . The single argument of the conformal eigenfunctions is the external coordinate of the Pomeron state. We have omitted the coordinates of the reggeised gluons contained in the Pomerons since they are integrated over to obtain the correlation function on the left-hand side. By writing down all the factors, one can obtain the following explicit form of the four-point function:

$$\begin{aligned} \left\langle E^{(\nu_a,0)*}(\rho_a) E^{(\nu_b,0)*}(\rho_b) E^{(\nu_c,0)*}(\rho_c) E^{(\nu_d,0)}(\rho_d) \right\rangle = \\ = \Psi(x, x^*; \{\nu_i\}) \left( \frac{|\rho_{ab}|^2 |\rho_{ac}|^2 |\rho_{ad}|^2}{|\rho_{bc}| |\rho_{bd}| |\rho_{cd}|} \right)^{-\frac{1}{3} + \frac{2}{3} i\nu_a} \left( \frac{|\rho_{ab}|^2 |\rho_{bc}|^2 |\rho_{bd}|^2}{|\rho_{ac}| |\rho_{ad}| |\rho_{cd}|} \right)^{-\frac{1}{3} + \frac{2}{3} i\nu_b} \\ \cdot \left( \frac{|\rho_{ac}|^2 |\rho_{bc}|^2 |\rho_{cd}|^2}{|\rho_{ab}| |\rho_{ad}| |\rho_{bd}|} \right)^{-\frac{1}{3} + \frac{2}{3} i\nu_c} \left( \frac{|\rho_{ad}|^2 |\rho_{bd}|^2 |\rho_{cd}|^2}{|\rho_{ab}| |\rho_{ac}| |\rho_{bc}|} \right)^{-\frac{1}{3} - \frac{2}{3} i\nu_d}. \end{aligned} \quad (59)$$

Now we rewrite the ratios in brackets as follows (shown here for the first expression):

$$\frac{|\rho_{ab}|^2 |\rho_{ac}|^2 |\rho_{ad}|^2}{|\rho_{bc}| |\rho_{bd}| |\rho_{cd}|} = \left| \frac{\rho_{ab}\rho_{cd}}{\rho_{ac}\rho_{bd}} \right| \left| \frac{\rho_{ab}\rho_{cd}}{\rho_{ad}\rho_{bc}} \right| \frac{|\rho_{ac}|^3 |\rho_{ad}|^3}{|\rho_{cd}|^3}. \quad (60)$$

The first of the anharmonic ratios appearing here is what we defined as  $x$  in Eq. (57), the second is  $x/(1-x)$ . We rewrite the following two factors in (59) analogously to (60), i.e. with the indices  $a, b$  and  $c$  permutated in order:  $a \rightarrow b \rightarrow c$ . Taking these three expressions together, one notices that the constant part of the exponents,  $-\frac{1}{3}$ , of the first three anharmonic ratios cancel. From the last factor in (59), we pull out the two different anharmonic ratios which have  $\rho_{ad}\rho_{bc}$  in the numerator, again analogously to (60). This leads to

$$\begin{aligned}
\langle \dots \rangle &= \Psi(x, x^*; \{\nu_i\}) \left| \frac{\rho_{ab}\rho_{cd}}{\rho_{ac}\rho_{bd}} \right|^{\frac{2}{3}i(\nu_a-\nu_c)} \left| \frac{\rho_{ab}\rho_{cd}}{\rho_{ad}\rho_{bc}} \right|^{\frac{1}{3}+\frac{2}{3}i(\nu_a-\nu_b+\nu_d)} \left| \frac{\rho_{ad}\rho_{bc}}{\rho_{ac}\rho_{bd}} \right|^{-\frac{1}{3}+\frac{2}{3}i(\nu_b-\nu_c-\nu_d)} \\
&\cdot \left( \frac{|\rho_{ac}||\rho_{ad}|}{|\rho_{cd}|} \right)^{-1+2i\nu_a} \left( \frac{|\rho_{ab}||\rho_{bd}|}{|\rho_{ad}|} \right)^{-1+2i\nu_b} \left( \frac{|\rho_{bc}||\rho_{cd}|}{|\rho_{bd}|} \right)^{-1+2i\nu_c} \left( \frac{|\rho_{bd}||\rho_{cd}|}{|\rho_{bc}|} \right)^{-1-2i\nu_d} \\
&= \Psi(x, x^*; \{\nu_i\}) |x|^{\frac{1}{3}+\frac{2}{3}i(2\nu_a-\nu_b-\nu_c+\nu_d)} |1-x|^{-\frac{2}{3}+\frac{2}{3}i(-\nu_a+2\nu_b-\nu_c-2\nu_d)} \cdot \\
&\cdot \left( \frac{|\rho_{ac}||\rho_{ad}|}{|\rho_{cd}|} \right)^{-1+2i\nu_a} \left( \frac{|\rho_{ab}||\rho_{bd}|}{|\rho_{ad}|} \right)^{-1+2i\nu_b} \left( \frac{|\rho_{bc}||\rho_{cd}|}{|\rho_{bd}|} \right)^{-1+2i\nu_c} \left( \frac{|\rho_{bd}||\rho_{cd}|}{|\rho_{bc}|} \right)^{-1-2i\nu_d}
\end{aligned} \tag{61}$$

Given a conformal four-point function, we can obtain the corresponding  $\Psi$  function by solving (57) for  $\Psi$ . After expressing the powers of  $|\rho_{ij}|$  in terms of  $x$  and of ratios of three  $|\rho_{ij}|$ s, we obtain the formula

$$\begin{aligned}
\Psi &= |x|^{-\frac{1}{3}+\frac{2}{3}i(-2\nu_a+\nu_b+\nu_c-\nu_d)} |1-x|^{\frac{2}{3}+\frac{2}{3}i(\nu_a-2\nu_b+\nu_c+2\nu_d)} \cdot \\
&\cdot \left( \frac{|\rho_{ac}||\rho_{ad}|}{|\rho_{cd}|} \right)^{1-2i\nu_a} \left( \frac{|\rho_{ab}||\rho_{bd}|}{|\rho_{ad}|} \right)^{1-2i\nu_b} \left( \frac{|\rho_{bc}||\rho_{cd}|}{|\rho_{bd}|} \right)^{1-2i\nu_c} \left( \frac{|\rho_{bd}||\rho_{cd}|}{|\rho_{bc}|} \right)^{1+2i\nu_d} \\
&\cdot \left\langle E^{(\nu_a,0)*}(\rho_a) E^{(\nu_b,0)*}(\rho_b) E^{(\nu_c,0)*}(\rho_c) E^{(\nu_d,0)}(\rho_d) \right\rangle.
\end{aligned} \tag{62}$$

From now on we will not write the arguments of  $\Psi$  explicitly any more. It depends on the  $\nu_i$  as well as on  $x$  and  $x^*$ .

### 3.3.2 The BFKL term

Since each of the integral expressions derived in Section 3.2 is a conformal four-point function, the  $\Psi$  function of the vertex can be written as a sum over five  $\Psi$  functions associated with the BFKL term and the four  $\alpha$  terms. They can be computed by inserting the integrals into Eq. (62). We will start by calculating the  $\Psi$  function of the BFKL term,  $\Psi_{\text{BFKL}}$ . Inserting (46) into the formula for  $\Psi$ , we get:

$$\begin{aligned}
\Psi_{\text{BFKL}} &= C \frac{g^6}{16} 4 \frac{2}{(2\pi)^3} \xi(\nu_d) (4\nu_d^2 + 1)^2 |x|^{-\frac{1}{3}+\frac{2}{3}i(-2\nu_a+\nu_b+\nu_c-\nu_d)} \cdot \\
&\cdot |1-x|^{\frac{2}{3}+\frac{2}{3}i(\nu_a-2\nu_b+\nu_c+2\nu_d)} \left( \frac{|\rho_{ac}||\rho_{ad}|}{|\rho_{cd}|} \right)^{1-2i\nu_a} \left( \frac{|\rho_{ab}||\rho_{bd}|}{|\rho_{ad}|} \right)^{1-2i\nu_b} \\
&\cdot \left( \frac{|\rho_{bc}||\rho_{cd}|}{|\rho_{bd}|} \right)^{1-2i\nu_c} \left( \frac{|\rho_{bd}||\rho_{cd}|}{|\rho_{bc}|} \right)^{1+2i\nu_d} \int \frac{d^2\rho_1 d^2\rho_2}{|\rho_{12}|^4} \left( \frac{|\rho_{12}|}{|\rho_{1a}||\rho_{2a}|} \right)^{1-2i\nu_a} \\
&\cdot \left( \frac{|\rho_{12}|}{|\rho_{1b}||\rho_{2b}|} \right)^{1-2i\nu_b} \left( \frac{|\rho_{12}|}{|\rho_{1c}||\rho_{2c}|} \right)^{1-2i\nu_c} \left( \frac{|\rho_{12}|}{|\rho_{1d}||\rho_{2d}|} \right)^{1+2i\nu_d} \\
&= C \frac{g^6}{16} 4 \frac{2}{(2\pi)^3} \xi(\nu_d) (4\nu_d^2 + 1)^2 |x|^{-\frac{1}{3}+\frac{2}{3}i(-2\nu_a+\nu_b+\nu_c-\nu_d)} \cdot \\
&\cdot |1-x|^{\frac{2}{3}+\frac{2}{3}i(\nu_a-2\nu_b+\nu_c+2\nu_d)} \int \frac{d^2\rho_1 d^2\rho_2}{|\rho_{12}|^4} \left( \frac{|\rho_{12}|}{|\rho_{1a}||\rho_{2a}|} \frac{|\rho_{ac}||\rho_{ad}|}{|\rho_{cd}|} \right)^{1-2i\nu_a} \\
&\cdot \left( \frac{|\rho_{12}|}{|\rho_{1b}||\rho_{2b}|} \frac{|\rho_{ab}||\rho_{bd}|}{|\rho_{ad}|} \right)^{1-2i\nu_b} \left( \frac{|\rho_{12}|}{|\rho_{1c}||\rho_{2c}|} \frac{|\rho_{bc}||\rho_{cd}|}{|\rho_{bd}|} \right)^{1-2i\nu_c}.
\end{aligned}$$

$$\begin{aligned}
& \cdot \left( \frac{|\rho_{12}|}{|\rho_{1d}||\rho_{2d}|} \frac{|\rho_{bd}||\rho_{cd}|}{|\rho_{bc}|} \right)^{1+2i\nu_d} \\
& = C \frac{g^6}{16} 4 \frac{2}{(2\pi)^3} \xi(\nu_d) (4\nu_d^2 + 1)^2 \Xi(-\nu_a, -\nu_b, -\nu_c, \nu_d; x, x^*), \tag{63}
\end{aligned}$$

where the last equality defines the function  $\Xi$ . Note that all the factors in (63) are conformally invariant by themselves. The function  $\Xi$  is defined as the integral multiplied with the powers of the anharmonic ratios. It was defined with the arguments  $-\nu_a, \dots, -\nu_c$ . Unlike a general four-point function, our four-point function contains three complex conjugated wave functions, so this notation facilitates comparison and generalisation of our result.

The function  $\Xi$  is symmetric under simultaneous exchange of the Pomeron coordinates and the  $\tilde{\nu}$ s ( $\tilde{\nu}_{a/b/c} = -\nu_{a/b/c}$ ,  $\tilde{\nu}_d = \nu_d$ ). This follows from the fact that both the part of the vertex without the  $\Psi$  function (see (57)) and the integral of the BFKL term (46) have this symmetry. Note that a permutation of the coordinates changes the anharmonic ratio which is the last argument of  $\Xi$ .

### 3.3.3 The $\alpha$ terms

In this section we will calculate the  $\Psi$  functions corresponding to the terms containing the function  $\alpha$ . We will see that they can be written in a form quite similar to  $\Psi_{\text{BFKL}}$ .

We will start with the term which arose from the set  $M$  having one element,  $V^{(1)}$ . It contained a sub-integral with an expression which had to be regularised. The same integral has already occurred in a term of the  $1 \rightarrow 2$  Pomeron vertex. The associated integral operator is conformally invariant and was found to have the eigenvalue  $1/2 \xi(\nu)$  [29],

$$\begin{aligned}
& \int d^2\rho_1 \left[ 2\pi \delta^2(\rho_{13}) \log \epsilon + \frac{|\rho_{23}|^2}{|\rho_{12}|^2 |\rho_{13}|^2} \theta \left( \frac{|\rho_{13}|}{|\rho_{12}|} - \epsilon \right) \right] \left( \frac{|\rho_{12}|}{|\rho_{1a}||\rho_{2a}|} \right)^{1-2i\nu_a} = \\
& = \frac{1}{2} \xi(\nu_a) \left( \frac{|\rho_{23}|}{|\rho_{2a}||\rho_{3a}|} \right)^{1-2i\nu_a} \tag{64}
\end{aligned}$$

Inserting this relation, we get for this part of the vertex:

$$\begin{aligned}
V_{\mathbb{P} \rightarrow 3\mathbb{P}}^{(1)} & = -C \frac{g^6}{16} 4 \frac{2}{(2\pi)^3} (4\nu_d^2 + 1)^2 \sum_{a \leftrightarrow b \leftrightarrow c} \int \frac{d^2\rho_2 d^2\rho_3}{|\rho_{23}|^4} \left( \frac{|\rho_{23}|}{|\rho_{2b}||\rho_{3b}|} \right)^{1-2i\nu_b} \cdot \\
& \cdot \left( \frac{|\rho_{23}|}{|\rho_{2c}||\rho_{3c}|} \right)^{1-2i\nu_c} \left( \frac{|\rho_{23}|}{|\rho_{2d}||\rho_{3d}|} \right)^{1+2i\nu_d} \frac{1}{2} \xi(\nu_a) \left( \frac{|\rho_{23}|}{|\rho_{2a}||\rho_{3a}|} \right)^{1-2i\nu_a} \\
& = -C \frac{g^6}{16} 4 \frac{2}{(2\pi)^3} (\xi(\nu_a) + \xi(\nu_b) + \xi(\nu_c)) (4\nu_d^2 + 1)^2 \int \frac{d^2\rho_2 d^2\rho_3}{|\rho_{23}|^4} \cdot \\
& \cdot \left( \frac{|\rho_{23}|}{|\rho_{2a}||\rho_{3a}|} \right)^{1-2i\nu_a} \left( \frac{|\rho_{23}|}{|\rho_{2b}||\rho_{3b}|} \right)^{1-2i\nu_b} \left( \frac{|\rho_{23}|}{|\rho_{2c}||\rho_{3c}|} \right)^{1-2i\nu_c} \left( \frac{|\rho_{23}|}{|\rho_{2d}||\rho_{3d}|} \right)^{1+2i\nu_d}. \tag{65}
\end{aligned}$$

Since the integrand except for the  $\xi$  function is symmetric in the Pomeron indices  $a$ ,  $b$  and  $c$ , we could remove the sum over the permutations and insert a sum over  $\xi$ s

instead. The result closely resembles the BFKL term (46), except for the sign and the argument of the  $\xi$  function. Therefore we can immediately write down the  $\Psi$  function of this part of the vertex,

$$\Psi_{(1)} = -C \frac{g^6}{16} 4 \frac{2}{(2\pi)^3} (\xi(\nu_a) + \xi(\nu_b) + \xi(\nu_c)) (4\nu_d^2 + 1)^2 \Xi(-\nu_a, -\nu_b, -\nu_c, \nu_d; x, x^*). \quad (66)$$

The next group of  $\alpha$  terms,  $V^{(2,1)}$  contains a new integral. We will see later that this integral occurs in none of the other terms. Therefore we will just write down  $\Psi_{(2,1)}$  without defining a function analogous to  $\Xi$ . Plugging (54) into (62), we get:

$$\begin{aligned} \Psi_{(2,1)} = & C \frac{g^6}{16} 4 \frac{2}{(2\pi)^3} (4\nu_d^2 + 1)^2 |x|^{-\frac{1}{3} + \frac{2}{3}i(-2\nu_a + \nu_b + \nu_c - \nu_d)} |1 - x|^{\frac{2}{3} + \frac{2}{3}i(\nu_a - 2\nu_b + \nu_c + 2\nu_d)} \cdot \\ & \cdot \left( \frac{|\rho_{ac}||\rho_{ad}|}{|\rho_{cd}|} \right)^{1-2i\nu_a} \left( \frac{|\rho_{ab}||\rho_{bd}|}{|\rho_{ad}|} \right)^{1-2i\nu_b} \left( \frac{|\rho_{bc}||\rho_{cd}|}{|\rho_{bd}|} \right)^{1-2i\nu_c} \left( \frac{|\rho_{bd}||\rho_{cd}|}{|\rho_{bc}|} \right)^{1+2i\nu_d} \cdot \\ & \cdot \sum_{a \leftrightarrow b \leftrightarrow c} \int d^2\rho_1 d^2\rho_2 \frac{1}{|\rho_{12}|^4} \left( \frac{|\rho_{12}|}{|\rho_{1a}||\rho_{2a}|} \right)^{1-2i\nu_a} \left( \frac{|\rho_{12}|}{|\rho_{1d}||\rho_{2d}|} \right)^{1+2i\nu_d} \cdot \\ & \cdot \int d^2\rho_3 \left[ 2\pi \delta^2(\rho_{23}) \log \epsilon + \frac{|\rho_{12}|^2}{|\rho_{13}|^2 |\rho_{23}|^2} \theta \left( \frac{|\rho_{23}|}{|\rho_{13}|} - \epsilon \right) \right] \left( \frac{|\rho_{13}|}{|\rho_{1b}||\rho_{3b}|} \right)^{1-2i\nu_b} \cdot \\ & \cdot \left( \frac{|\rho_{13}|}{|\rho_{1c}||\rho_{3c}|} \right)^{1-2i\nu_c}. \end{aligned} \quad (67)$$

There remain the integrals  $V^{(2,2)}$  and  $V^{(3)}$ . Looking at the formulas (55) and (56), one can see that they are very similar. One has to be aware that the only distinction between different terms is the number of Pomerons attached to a given pair of coordinates, (12), (13) or (23). Which of the three Pomerons  $a$ ,  $b$  and  $c$  is attached to which does not matter since all permutations are summed up. Also, the indices of the integration variables are immaterial because renaming them changes nothing. Only one pair of indices is distinguished from the others by the fact that the upper Pomeron with index  $d$  is attached to it.

Taking all this into account, the only difference between  $V^{(2,2)}$  and  $V^{(3)}$  is the following: In  $V^{(2,2)}$ , each of the three Pomerons attached to the vertex from below has a different pair of coordinates as their arguments. In  $V^{(3)}$ , none of the lower Pomerons has the same pair of coordinate arguments as the upper ( $d$ ) Pomeron. Instead, two of them have the same pair of arguments. (This can also be seen in the graphical representation in Figure 3 when one realises that the upper two lines have the same coordinates as the outer lines below.) This implies that  $V^{(3)}$  can be obtained from  $V^{(2,2)}$  by exchanging  $\rho_d$  with the external coordinate of one of the two lower Pomerons which have the same arguments ( $\rho_b$  or  $\rho_c$  in (56)), and simultaneously exchanging  $\nu_d \leftrightarrow -\nu_b$  or  $\nu_d \leftrightarrow -\nu_c$ , respectively. Then the Pomeron  $b$  resp.  $c$  has the arguments which previously none of the lower Pomerons had, and Pomeron  $d$  has the same arguments as one of the lower Pomerons. This is exactly the situation in  $V^{(2,2)}$  (modulo permutation of the lower Pomerons and/or renaming of the integration variables). We hence have the relation

$$V_{\mathbb{P} \rightarrow 3\mathbb{P}}^{(3)} \xleftrightarrow{\rho_d \leftrightarrow \rho_b, \nu_d \leftrightarrow -\nu_b} V_{\mathbb{P} \rightarrow 3\mathbb{P}}^{(2,2)}. \quad (68)$$



Therefore it can already be stated without any calculation that  $V^{(2,2)}$  and  $V^{(3)}$  lead to the same type of integral.

In the following, we will calculate  $\Psi_{(3)}$ .  $\Psi_{(2,2)}$  can then be obtained by exchanging the coordinates and conformal dimension according to (68). Inserting (56) into the formula for  $\Psi$ , Eq. (62), we get:

$$\begin{aligned}
\Psi_{(3)} &= -C \frac{g^6}{16} 4 \frac{2}{(2\pi)^3} (4\nu_d^2 + 1)^2 |x|^{-\frac{1}{3} + \frac{2}{3}i(-2\nu_a + \nu_b + \nu_c - \nu_d)} |1 - x|^{\frac{2}{3} + \frac{2}{3}i(\nu_a - 2\nu_b + \nu_c + 2\nu_d)} \cdot \\
&\quad \cdot \left( \frac{|\rho_{ac}||\rho_{ad}|}{|\rho_{cd}|} \right)^{1-2i\nu_a} \left( \frac{|\rho_{ab}||\rho_{bd}|}{|\rho_{ad}|} \right)^{1-2i\nu_b} \left( \frac{|\rho_{bc}||\rho_{cd}|}{|\rho_{bd}|} \right)^{1-2i\nu_c} \left( \frac{|\rho_{bd}||\rho_{cd}|}{|\rho_{bc}|} \right)^{1+2i\nu_d} \cdot \\
&\quad \cdot \sum_{a \leftrightarrow b \leftrightarrow c} \int \frac{d^2\rho_1 d^2\rho_2 d^2\rho_3}{|\rho_{12}|^2 |\rho_{13}|^2 |\rho_{23}|^2} \left( \frac{|\rho_{12}|}{|\rho_{1a}||\rho_{2a}|} \right)^{1-2i\nu_a} \left( \frac{|\rho_{13}|}{|\rho_{1b}||\rho_{3b}|} \right)^{1-2i\nu_b} \cdot \\
&\quad \cdot \left( \frac{|\rho_{13}|}{|\rho_{1c}||\rho_{3c}|} \right)^{1-2i\nu_c} \left( \frac{|\rho_{23}|}{|\rho_{2d}||\rho_{3d}|} \right)^{1+2i\nu_d} \\
&= -C \frac{g^6}{16} 4 \frac{2}{(2\pi)^3} (4\nu_d^2 + 1)^2 \sum_{a \leftrightarrow b \leftrightarrow c} |x|^{-\frac{1}{3} + \frac{2}{3}i(-2\nu_a + \nu_b + \nu_c - \nu_d)} \cdot \\
&\quad \cdot |1 - x|^{\frac{2}{3} + \frac{2}{3}i(\nu_a - 2\nu_b + \nu_c + 2\nu_d)} \int \frac{d^2\rho_1 d^2\rho_2 d^2\rho_3}{|\rho_{12}|^2 |\rho_{13}|^2 |\rho_{23}|^2} \left( \frac{|\rho_{12}|}{|\rho_{1a}||\rho_{2a}|} \frac{|\rho_{ac}||\rho_{ad}|}{|\rho_{cd}|} \right)^{1-2i\nu_a} \cdot \\
&\quad \cdot \left( \frac{|\rho_{13}|}{|\rho_{1b}||\rho_{3b}|} \frac{|\rho_{ab}||\rho_{bd}|}{|\rho_{ad}|} \right)^{1-2i\nu_b} \left( \frac{|\rho_{13}|}{|\rho_{1c}||\rho_{3c}|} \frac{|\rho_{bc}||\rho_{cd}|}{|\rho_{bd}|} \right)^{1-2i\nu_c} \cdot \\
&\quad \cdot \left( \frac{|\rho_{23}|}{|\rho_{2d}||\rho_{3d}|} \frac{|\rho_{bd}||\rho_{cd}|}{|\rho_{bc}|} \right)^{1+2i\nu_d} \\
&= -C \frac{g^6}{16} 4 \frac{2}{(2\pi)^3} (4\nu_d^2 + 1)^2 \sum_{a \leftrightarrow b \leftrightarrow c} \Upsilon(-\nu_b, -\nu_c, -\nu_a, \nu_d; x, x^*) \cdot \tag{69}
\end{aligned}$$

The step from the first to the second expression is not trivial. It is possible only because the vertex without the  $\Psi$  function is invariant under permutations of the Pomerons  $a$ ,  $b$  and  $c$ , as can be seen from (57). (In fact it is symmetric under all permutations of conformal fields if one takes care of the different sign of  $\nu_d$ .) It is this part of the vertex which we have written into the sum over the permutations, even though the symmetry is not obvious any more. The sum over the permutations also extends to  $x$  in the sense that it is transformed into a different anharmonic ratio by a permutation of the coordinates. In fact, all six anharmonic ratios occur in the sum, some with a minus sign.

The function  $\Upsilon$  in (69) is defined as follows:

$$\begin{aligned}
\Upsilon(-\nu_b, -\nu_c, -\nu_a, \nu_d; x, x^*) &= |x|^{-\frac{1}{3} + \frac{2}{3}i(-2\nu_a + \nu_b + \nu_c - \nu_d)} |1 - x|^{\frac{2}{3} + \frac{2}{3}i(\nu_a - 2\nu_b + \nu_c + 2\nu_d)} \cdot \\
&\quad \cdot \int \frac{d^2\rho_1 d^2\rho_2 d^2\rho_3}{|\rho_{12}|^2 |\rho_{13}|^2 |\rho_{23}|^2} \left( \frac{|\rho_{12}|}{|\rho_{1a}||\rho_{2a}|} \frac{|\rho_{ac}||\rho_{ad}|}{|\rho_{cd}|} \right)^{1-2i\nu_a} \left( \frac{|\rho_{13}|}{|\rho_{1b}||\rho_{3b}|} \frac{|\rho_{ab}||\rho_{bd}|}{|\rho_{ad}|} \right)^{1-2i\nu_b} \cdot \\
&\quad \cdot \left( \frac{|\rho_{13}|}{|\rho_{1c}||\rho_{3c}|} \frac{|\rho_{bc}||\rho_{cd}|}{|\rho_{bd}|} \right)^{1-2i\nu_c} \left( \frac{|\rho_{23}|}{|\rho_{2d}||\rho_{3d}|} \frac{|\rho_{bd}||\rho_{cd}|}{|\rho_{bc}|} \right)^{1+2i\nu_d} \cdot \tag{70}
\end{aligned}$$

We have defined it so that the conformal dimensions of the two Pomerons with the same coordinate arguments come first. It is symmetric in these first two arguments provided the corresponding coordinates are exchanged as well, which leads to a different anharmonic ratio,  $1/x$  instead of  $x$ ,

$$\Upsilon(-\nu_b, -\nu_c, -\nu_a, \nu_d; x, x^*) = \Upsilon(-\nu_c, -\nu_b, -\nu_a, \nu_d; \frac{1}{x}, \frac{1}{x^*}). \quad (71)$$

The conformally invariant function  $\Psi_{(2,2)}$  corresponding to  $V^{(2,2)}$  can be obtained from  $\Psi_{(3)}$  by way of (68). The only slight difficulty is the anharmonic ratio  $x$ . Exchanging the coordinates  $\rho_d \leftrightarrow \rho_b$  also changes the anharmonic ratio on which  $\Upsilon$  still depends,

$$x = \frac{\rho_{ab}\rho_{cd}}{\rho_{ac}\rho_{bd}} \longrightarrow \frac{\rho_{ad}\rho_{bc}}{\rho_{ac}\rho_{bd}} = 1 - x. \quad (72)$$

Therefore we obtain for  $\Psi_{(2,2)}$

$$\Psi_{(2,2)} = C \frac{g^6}{16} 4 \frac{2}{(2\pi)^3} (4\nu_d^2 + 1)^2 \sum_{a \leftrightarrow b \leftrightarrow c} \Upsilon(-\nu_d, -\nu_c, -\nu_a, \nu_b; 1 - x, 1 - x^*). \quad (73)$$

## 4 Summary and Conclusions

In this paper we have calculated the perturbative  $1 \rightarrow 3$  Pomeron vertex in the colour glass condensate. We have used the framework of the extended GLLA which is particularly well suited for the calculation of multi-Pomeron vertices. The  $1 \rightarrow 3$  Pomeron vertex is obtained by projecting the  $2 \rightarrow 6$  reggeised gluon vertex onto BFKL Pomeron states. The resulting  $1 \rightarrow 3$  Pomeron vertex is local in rapidity. In the present paper we have taken into account only Pomeron states with conformal spin  $n = 0$  which are the leading states at high energies. It is in principle straightforward to extend our calculation to states with nonvanishing conformal spin.

Let us now summarize the result of the calculation of the  $1 \rightarrow 3$  Pomeron vertex performed in the previous section. We have found that the  $1 \rightarrow 3$  Pomeron vertex has the form of a conformal four-point function,

$$V_{\mathbb{P} \rightarrow 3\mathbb{P}}(\{\rho_i\}; \{\nu_i\}) = \Psi(x, x^*; \{\nu_i\}) \prod_{i < j} |\rho_{ij}|^{2i(-\tilde{\nu}_i - \tilde{\nu}_j + \frac{1}{3} \sum_k \tilde{\nu}_k)}, \quad (74)$$

where the  $\rho_i$  are the coordinates of the four Pomerons in impact parameter space,  $x = (\rho_{ab}\rho_{cd})/(\rho_{ac}\rho_{bd})$ , and we have  $\tilde{\nu}_i = -\nu_i$  for  $i = a, b, c$  and  $\tilde{\nu}_d = \nu_d$ .

The freedom which remains in the otherwise fixed form of the vertex, the function  $\Psi$ , can be written as a sum of five terms:

$$\begin{aligned} \Psi(x, x^*; \{\nu_i\}) &= \Psi_{\text{BFKL}}(x, x^*; \{\nu_i\}) + \Psi_{(1)}(x, x^*; \{\nu_i\}) \\ &+ \Psi_{(2,1)}(x, x^*; \{\nu_i\}) + \Psi_{(2,2)}(x, x^*; \{\nu_i\}) + \Psi_{(3)}(x, x^*; \{\nu_i\}). \end{aligned} \quad (75)$$

These five terms have the following form:

$$\Psi_{\text{BFKL}}(x, x^*; \{\nu_i\}) = C \frac{g^6}{2(2\pi)^3} \xi(\nu_d) (4\nu_d^2 + 1)^2 \Xi(-\nu_a, -\nu_b, -\nu_c, \nu_d; x, x^*) \quad (76)$$

$$\Psi_{(1)}(x, x^*; \{\nu_i\}) = -C \frac{g^6}{2(2\pi)^3} (\xi(\nu_a) + \xi(\nu_b) + \xi(\nu_c)) (4\nu_d^2 + 1)^2 \cdot \Xi(-\nu_a, -\nu_b, -\nu_c, \nu_d; x, x^*) \quad (77)$$

$$\begin{aligned} \Psi_{(2,1)}(x, x^*; \{\nu_i\}) = & C \frac{g^6}{2(2\pi)^3} (4\nu_d^2 + 1)^2 |x|^{-\frac{1}{3} + \frac{2}{3}i(-2\nu_a + \nu_b + \nu_c - \nu_d)} \cdot \\ & \cdot |1 - x|^{\frac{2}{3} + \frac{2}{3}i(\nu_a - 2\nu_b + \nu_c + 2\nu_d)} \left( \frac{|\rho_{ac}||\rho_{ad}|}{|\rho_{cd}|} \right)^{1-2i\nu_a} \left( \frac{|\rho_{ab}||\rho_{bd}|}{|\rho_{ad}|} \right)^{1-2i\nu_b} \cdot \\ & \cdot \left( \frac{|\rho_{bc}||\rho_{cd}|}{|\rho_{bd}|} \right)^{1-2i\nu_c} \left( \frac{|\rho_{bd}||\rho_{cd}|}{|\rho_{bc}|} \right)^{1+2i\nu_d} \sum_{a \leftrightarrow b \leftrightarrow c} \int d^2\rho_1 d^2\rho_2 \frac{1}{|\rho_{12}|^4} \cdot \\ & \cdot \left( \frac{|\rho_{12}|}{|\rho_{1a}||\rho_{2a}|} \right)^{1-2i\nu_a} \left( \frac{|\rho_{12}|}{|\rho_{1d}||\rho_{2d}|} \right)^{1+2i\nu_d} \int d^2\rho_3 \left[ 2\pi \delta^2(\rho_{23}) \log \epsilon \right. \\ & \left. + \frac{|\rho_{12}|^2}{|\rho_{13}|^2 |\rho_{23}|^2} \theta \left( \frac{|\rho_{23}|}{|\rho_{13}|} - \epsilon \right) \right] \left( \frac{|\rho_{13}|}{|\rho_{1b}||\rho_{3b}|} \right)^{1-2i\nu_b} \left( \frac{|\rho_{13}|}{|\rho_{1c}||\rho_{3c}|} \right)^{1-2i\nu_c} \quad (78) \end{aligned}$$

$$\Psi_{(2,2)}(x, x^*; \{\nu_i\}) = C \frac{g^6}{2(2\pi)^3} (4\nu_d^2 + 1)^2 \sum_{a \leftrightarrow b \leftrightarrow c} \Upsilon(-\nu_d, -\nu_c, -\nu_a, \nu_b; 1-x, 1-x^*) \quad (79)$$

$$\Psi_{(3)}(x, x^*; \{\nu_i\}) = -C \frac{g^6}{2(2\pi)^3} (4\nu_d^2 + 1)^2 \sum_{a \leftrightarrow b \leftrightarrow c} \Upsilon(-\nu_b, -\nu_c, -\nu_a, \nu_d; x, x^*) \cdot \quad (80)$$

We recall that the colour constant  $C$  has for general  $N_c$  the form

$$C = \frac{1}{N_c} (N_c^2 - 4)(N_c^2 - 1). \quad (81)$$

The sums in  $\Psi_{(2,1)}$ ,  $\Psi_{(2,2)}$  and  $\Psi_{(3)}$  run over all six simultaneous permutations of the conformal dimensions  $\nu_{a/b/c}$  and the corresponding coordinates  $\rho_{a/b/c}$ . That entails that  $x$  is replaced by a different cross ratio according to the permutation of the  $\rho$ s. The two integral expressions  $\Xi$  and  $\Upsilon$  in the expressions above are defined as

$$\begin{aligned} \Xi(-\nu_a, -\nu_b, -\nu_c, \nu_d; x, x^*) = & |x|^{-\frac{1}{3} + \frac{2}{3}i(-2\nu_a + \nu_b + \nu_c - \nu_d)} |1 - x|^{\frac{2}{3} + \frac{2}{3}i(\nu_a - 2\nu_b + \nu_c + 2\nu_d)} \cdot \\ & \cdot \int \frac{d^2\rho_1 d^2\rho_2}{|\rho_{12}|^4} \left( \frac{|\rho_{12}|}{|\rho_{1a}||\rho_{2a}|} \frac{|\rho_{ac}||\rho_{ad}|}{|\rho_{cd}|} \right)^{1-2i\nu_a} \left( \frac{|\rho_{12}|}{|\rho_{1b}||\rho_{2b}|} \frac{|\rho_{ab}||\rho_{bd}|}{|\rho_{ad}|} \right)^{1-2i\nu_b} \cdot \\ & \cdot \left( \frac{|\rho_{12}|}{|\rho_{1c}||\rho_{2c}|} \frac{|\rho_{bc}||\rho_{cd}|}{|\rho_{bd}|} \right)^{1-2i\nu_c} \left( \frac{|\rho_{12}|}{|\rho_{1d}||\rho_{2d}|} \frac{|\rho_{bd}||\rho_{cd}|}{|\rho_{bc}|} \right)^{1+2i\nu_d} \quad (82) \end{aligned}$$

$$\begin{aligned} \Upsilon(-\nu_b, -\nu_c, -\nu_a, \nu_d; x, x^*) = & |x|^{-\frac{1}{3} + \frac{2}{3}i(-2\nu_a + \nu_b + \nu_c - \nu_d)} |1 - x|^{\frac{2}{3} + \frac{2}{3}i(\nu_a - 2\nu_b + \nu_c + 2\nu_d)} \cdot \\ & \cdot \int \frac{d^2\rho_1 d^2\rho_2 d^2\rho_3}{|\rho_{12}|^2 |\rho_{13}|^2 |\rho_{23}|^2} \left( \frac{|\rho_{12}|}{|\rho_{1a}||\rho_{2a}|} \frac{|\rho_{ac}||\rho_{ad}|}{|\rho_{cd}|} \right)^{1-2i\nu_a} \left( \frac{|\rho_{13}|}{|\rho_{1b}||\rho_{3b}|} \frac{|\rho_{ab}||\rho_{bd}|}{|\rho_{ad}|} \right)^{1-2i\nu_b} \cdot \\ & \cdot \left( \frac{|\rho_{13}|}{|\rho_{1c}||\rho_{3c}|} \frac{|\rho_{bc}||\rho_{cd}|}{|\rho_{bd}|} \right)^{1-2i\nu_c} \left( \frac{|\rho_{23}|}{|\rho_{2d}||\rho_{3d}|} \frac{|\rho_{bd}||\rho_{cd}|}{|\rho_{bc}|} \right)^{1+2i\nu_d} \cdot \quad (83) \end{aligned}$$

Note that all terms of the  $1 \rightarrow 3$  Pomeron vertex calculated here are of the same order in powers of  $N_c$ . This is in contrast to the  $1 \rightarrow 2$  Pomeron vertex in which there

are two contributions one of which is suppressed by two powers of  $N_c$  with respect to the other.

We should point out again that we have only calculated the contribution to the  $1 \rightarrow 3$  Pomeron vertex coming from the  $2 \rightarrow 6$  gluon vertex. We expect that there are also other contributions to this vertex from the reggeising terms in the six-gluon amplitude which need to be computed in order to obtain a full picture of the vertex. First steps of that calculation have been performed in [35].

The  $1 \rightarrow 3$  Pomeron vertex gives an additional contribution to the  $t$ -channel evolution of hadronic scattering processes at high energy. It would of course be very important to determine the relative importance of this vertex with respect to the usual fan diagrams in which the transition from one to three Pomerons occurs only via the iteration of the  $1 \rightarrow 2$  Pomeron vertex. In the expansion in  $N_c$  the direct  $1 \rightarrow 3$  Pomeron vertex is clearly suppressed with respect to the transition via the iterated  $1 \rightarrow 2$  Pomeron vertex, i.e. with respect to the corresponding fan diagram. But in order to determine the relative importance of the  $1 \rightarrow 3$  Pomeron one also has to consider its numerical value which, if found to be large, can potentially compensate the suppression due to factors of  $N_c$ . In this context one also has to consider the additional contributions to the  $1 \rightarrow 3$  Pomeron vertex coming from the reggeising terms in the six-gluon amplitude, which we have mentioned above and which have not yet been calculated. These contributions are not necessarily of the same order in the  $N_c$  expansion, in particular they can be less suppressed with respect to the iterated  $1 \rightarrow 2$  Pomeron vertex in the fan diagrams. These issues need to be studied in detail before the question of the phenomenological relevance of the  $1 \rightarrow 3$  Pomeron vertex can be answered.

As already pointed out it would be important to calculate the numerical value of the perturbative  $1 \rightarrow 3$  Pomeron vertex at least for the leading Pomeron states with  $h = 1/2$ . The integral expressions occurring in the vertex are in principle similar to those in the  $1 \rightarrow 2$  Pomeron vertex, which have been computed in [46]. The problem of computing the value of the  $1 \rightarrow 3$  Pomeron vertex, although it is clearly more complicated, can probably be approached with the same techniques.

The  $2 \rightarrow 4$  and the  $2 \rightarrow 6$  gluon vertex in the ELLA have a very similar structure which is most conveniently expressed in terms of the function  $G$ . Based on this structure it has been conjectured that also higher  $2 \rightarrow 2n$  gluon vertices exist for arbitrary  $n$  [34]. According to their conjectured momentum structure it appears likely that they also give rise to higher  $1 \rightarrow n$  Pomeron vertices which are local in rapidity. But we have seen above that also the colour structure of the  $2 \rightarrow 6$  gluon vertex was crucial for identifying the terms contributing to the  $1 \rightarrow 3$  Pomeron vertex. In order to establish the existence of general  $1 \rightarrow n$  Pomeron vertices one would therefore not only have to prove the conjectured momentum structure. In addition it would be necessary to determine also the explicit colour tensors of the  $2 \rightarrow 2n$  gluon vertices.

An important conceptual implication of our result is that it indicates an inequivalence of the ELLA and the dipole picture of high energy scattering occurring when one goes beyond the approximation of fan diagrams involving only the  $1 \rightarrow 2$  Pomeron vertex. We have found that in the ELLA a  $1 \rightarrow 3$  Pomeron vertex exists which is local in rapidity, whereas in the dipole picture such a local vertex is absent according to [30]. We also find that our formula for the  $1 \rightarrow 3$  Pomeron vertex does not coincide with the form conjectured for this vertex in [50] based on a generalization of the  $1 \rightarrow 2$

Pomeron vertex in the dipole picture. Nevertheless, it appears possible that the two are related to each other in suitable limits or via duality or bootstrap relations. Also here the other contributions from the reggeising parts of the six-gluon amplitude to the  $1 \rightarrow 3$  Pomeron vertex might be relevant. It would of course be very interesting to study whether the  $1 \rightarrow 3$  Pomeron vertex found in the present paper can also be obtained in other approaches to high energy QCD. In this way one can hope to learn about the relations and characteristic differences between different approaches to the physics of the colour glass condensate.

## Acknowledgements

We would like to thank Jochen Bartels, Gregory Korchemsky, and Robi Peschanski for helpful discussions.

## Appendix

### Derivatives of the conformal eigenfunctions $E^{(\nu,n)}$

When proving the conformal transformation properties of the  $G$  function we have used the explicit form of derivatives of the conformal eigenfunction  $E^{(\nu,n)}$ . These derivatives will be calculated in this appendix.

The starting point is the explicit form of the conformal eigenfunction  $E^{(\nu,n)}$  of the BFKL kernel in position space as given in (33).  $\rho_a$  in that formula is the external coordinate of the Pomeron state.

The differential operators which occur in the  $G$  function are:  $\Delta_1 \Delta_2$ ,  $\nabla_1 \Delta_2$  and a single  $\Delta_1$ . Expressed as derivatives with respect to the complex coordinates, they become:  $16 \partial_1 \partial_1^* \partial_2 \partial_2^*$ ,  $8 \partial_1^* \partial_2 \partial_2^*$  and  $4 \partial_1 \partial_1^*$ , respectively. We can completely separate the conjugated from the unconjugated coordinates.

We first calculate the gradient with respect to one coordinate of the eigenfunction  $E^{(\nu,n)}$ .

$$\begin{aligned} \nabla_1 E^{(\nu,n)}(\rho_1, \rho_2) &= 2 \partial_1^* E^{(\nu,n)}(\rho_1, \rho_2) = 2 \left( \frac{\rho_{12}}{\rho_{1a} \rho_{2a}} \right)^{\frac{1+n}{2} + i\nu} \partial_1^* \left( \frac{\rho_{12}^*}{\rho_{1a}^* \rho_{2a}^*} \right)^{\frac{1-n}{2} + i\nu} \\ &= 2 \left( \frac{\rho_{12}}{\rho_{1a} \rho_{2a}} \right)^{\frac{1+n}{2} + i\nu} \left( \frac{1-n}{2} + i\nu \right) \left( \frac{\rho_{12}^*}{\rho_{1a}^* \rho_{2a}^*} \right)^{-\frac{1-n}{2} + i\nu} \frac{1}{\rho_{1a}^*{}^2} \\ &= (1-n+2i\nu) \frac{\rho_{2a}^*}{\rho_{1a}^* \rho_{12}^*} E^{(\nu,n)}(\rho_1, \rho_2). \end{aligned} \quad (84)$$

Performing the differentiation with respect to the non-conjugated coordinate yields an analogous result, and similar results hold for the other coordinate,

$$\nabla_1^* E^{(\nu,n)}(\rho_1, \rho_2) = (1+n+2i\nu) \frac{\rho_{2a}}{\rho_{1a} \rho_{12}} E^{(\nu,n)}(\rho_1, \rho_2) \quad (85)$$

$$\nabla_2 E^{(\nu,n)}(\rho_1, \rho_2) = -(1-n+2i\nu) \frac{\rho_{1a}^*}{\rho_{2a}^* \rho_{12}^*} E^{(\nu,n)}(\rho_1, \rho_2) \quad (86)$$

$$\nabla_2^* E^{(\nu,n)}(\rho_1, \rho_2) = -(1+n+2i\nu) \frac{\rho_{1a}}{\rho_{2a} \rho_{12}} E^{(\nu,n)}(\rho_1, \rho_2). \quad (87)$$

The derivatives with respect to  $\rho_2$  get a minus sign because the result is expressed in  $\rho_{12}$  instead of  $\rho_{21}$ .

Having derived the gradient, we can immediately give the Laplacians of a Pomeron wave function  $E^{(\nu,n)}$ . Since the differentiations with respect to (un)conjugated variables add only factors of variables of the same type, the two differentiations contained in a Laplacian are independent. We obtain

$$\Delta_1 E^{(\nu,n)}(\rho_1, \rho_2) = ((1 + 2i\nu)^2 - n^2) \frac{|\rho_{2a}|^2}{|\rho_{1a}|^2 |\rho_{12}|^2} E^{(\nu,n)}(\rho_1, \rho_2) \quad (88)$$

$$\Delta_2 E^{(\nu,n)}(\rho_1, \rho_2) = ((1 + 2i\nu)^2 - n^2) \frac{|\rho_{1a}|^2}{|\rho_{2a}|^2 |\rho_{12}|^2} E^{(\nu,n)}(\rho_1, \rho_2). \quad (89)$$

The combination of a gradient and a Laplacian requires some more work. Here the gradient affects also the additional coordinate moduli in (89). In this case we find

$$\begin{aligned} \nabla_1 \Delta_2 E^{(\nu,n)}(\rho_1, \rho_2) &= \nabla_1 ((1 + 2i\nu)^2 - n^2) \frac{|\rho_{1a}|^2}{|\rho_{2a}|^2 |\rho_{12}|^2} E^{(\nu,n)}(\rho_1, \rho_2) \\ &= ((1 + 2i\nu)^2 - n^2) \left( 2 \left( \partial_1^* \frac{|\rho_{1a}|^2}{|\rho_{2a}|^2 |\rho_{12}|^2} \right) \right. \\ &\quad \left. + \frac{|\rho_{1a}|^2}{|\rho_{2a}|^2 |\rho_{12}|^2} (1 - n + 2i\nu) \frac{\rho_{2a}^*}{\rho_{1a}^* \rho_{12}^*} \right) E^{(\nu,n)}(\rho_1, \rho_2). \end{aligned} \quad (90)$$

The derivative of the first factor becomes

$$\partial_1^* \frac{|\rho_{1a}|^2}{|\rho_{2a}|^2 |\rho_{12}|^2} = \frac{\rho_{1a}}{|\rho_{2a}|^2 \rho_{12}} \partial_1^* \frac{\rho_{1a}^*}{\rho_{12}^*} = \frac{|\rho_{1a}|^2}{|\rho_{2a}|^2 |\rho_{12}|^2} \frac{-\rho_{2a}^*}{\rho_{1a}^* \rho_{12}^*}. \quad (91)$$

This term can easily be added to the derivative of the second factor, giving the constant prefactor  $(-1 - n + 2i\nu)$ . After factorising the prefactor of (89) and combining it with the new factor, we obtain the result:

$$\begin{aligned} \nabla_1 \Delta_2 E^{(\nu,n)}(\rho_1, \rho_2) &= \\ &= -(4\nu^2 + (n+1)^2)(1 - n + 2i\nu) \frac{\rho_{2a}^*}{\rho_{1a}^* \rho_{12}^*} \frac{|\rho_{1a}|^2}{|\rho_{2a}|^2 |\rho_{12}|^2} E^{(\nu,n)}(\rho_1, \rho_2). \end{aligned} \quad (92)$$

The additional differentiation necessary to apply a double Laplacian to  $E^{(\nu,n)}$  is again independent of the one just performed and can be done analogously. The moduli of  $\rho_{1a}$  and  $\rho_{2a}$  then cancel out. The result is

$$\Delta_1 \Delta_2 E^{(\nu,n)}(\rho_1, \rho_2) = (4\nu^2 + (n+1)^2)(4\nu^2 + (n-1)^2) \frac{1}{|\rho_{12}|^4} E^{(\nu,n)}(\rho_1, \rho_2). \quad (93)$$

## References

- [1] L. D. McLerran and R. Venugopalan, Phys. Rev. D **49** (1994) 3352 [arXiv:hep-ph/9311205].
- [2] L. D. McLerran and R. Venugopalan, Phys. Rev. D **49** (1994) 2233 [arXiv:hep-ph/9309289].

- [3] L. D. McLerran and R. Venugopalan, Phys. Rev. D **50** (1994) 2225 [arXiv:hep-ph/9402335].
- [4] J. Jalilian-Marian, A. Kovner, L. D. McLerran and H. Weigert, Phys. Rev. D **55** (1997) 5414 [arXiv:hep-ph/9606337].
- [5] E. Iancu, A. Leonidov and L. D. McLerran, Nucl. Phys. A **692** (2001) 583 [arXiv:hep-ph/0011241].
- [6] E. Ferreira, E. Iancu, A. Leonidov and L. McLerran, Nucl. Phys. A **703** (2002) 489 [arXiv:hep-ph/0109115].
- [7] E. Iancu and R. Venugopalan, arXiv:hep-ph/0303204.
- [8] I. Balitsky, Nucl. Phys. B **463** (1996) 99 [arXiv:hep-ph/9509348].
- [9] I. Balitsky, Phys. Rev. Lett. **81** (1998) 2024 [arXiv:hep-ph/9807434].
- [10] I. Balitsky, Phys. Rev. D **60** (1999) 014020 [arXiv:hep-ph/9812311].
- [11] I. Balitsky, Phys. Lett. B **518** (2001) 235 [arXiv:hep-ph/0105334].
- [12] I. I. Balitsky and A. V. Belitsky, Nucl. Phys. B **629** (2002) 290 [arXiv:hep-ph/0110158].
- [13] J. P. Blaizot, E. Iancu and H. Weigert, Nucl. Phys. A **713** (2003) 441 [arXiv:hep-ph/0206279].
- [14] Y. V. Kovchegov, Phys. Rev. D **60** (1999) 034008 [arXiv:hep-ph/9901281].
- [15] A. H. Mueller, Nucl. Phys. B **415** (1994) 373.
- [16] A. H. Mueller and B. Patel, Nucl. Phys. B **425** (1994) 471 [arXiv:hep-ph/9403256].
- [17] A. H. Mueller, Nucl. Phys. B **437** (1995) 107 [arXiv:hep-ph/9408245].
- [18] Z. Chen and A. H. Mueller, Nucl. Phys. B **451** (1995) 579.
- [19] E. A. Kuraev, L. N. Lipatov and V. S. Fadin, Sov. Phys. JETP **45** (1977) 199 [Zh. Eksp. Teor. Fiz. **72** (1977) 377].
- [20] I. I. Balitsky and L. N. Lipatov, Sov. J. Nucl. Phys. **28** (1978) 822 [Yad. Fiz. **28** (1978) 1597].
- [21] J. Bartels, Nucl. Phys. B **175** (1980) 365.
- [22] J. Kwieciński and M. Praszalowicz, Phys. Lett. B **94** (1980) 413.
- [23] J. Bartels, Nucl. Phys. B **151** (1979) 293.
- [24] J. Bartels, DESY 91-074 (unpublished)
- [25] J. Bartels, Phys. Lett. B **298** (1993) 204.
- [26] J. Bartels, Z. Phys. C **60** (1993) 471.

- [27] J. Bartels and M. Wüsthoff, Z. Phys. C **66** (1995) 157.
- [28] J. Bartels, L. N. Lipatov and M. Wüsthoff, Nucl. Phys. B **464** (1996) 298 [arXiv:hep-ph/9509303].
- [29] H. Lotter, Ph.D. Thesis, Hamburg University 1996, DESY 96-262, arXiv:hep-ph/9705288.
- [30] M. A. Braun and G. P. Vacca, Eur. Phys. J. C **6** (1999) 147 [arXiv:hep-ph/9711486].
- [31] J. Bartels and C. Ewerz, JHEP **9909** (1999) 026 [arXiv:hep-ph/9908454].
- [32] C. Ewerz, Phys. Lett. B **472** (2000) 135 [arXiv:hep-ph/9911225].
- [33] C. Ewerz, JHEP **0104** (2001) 031 [arXiv:hep-ph/0103260].
- [34] C. Ewerz, Phys. Lett. B **512** (2001) 239 [arXiv:hep-ph/0105181].
- [35] V. Schatz, Ph.D. Thesis, Heidelberg University 2003, HD-THEP-03-21, arXiv:hep-ph/0307326.
- [36] E. Ferreiro, E. Iancu, K. Itakura and L. McLerran, Nucl. Phys. A **710** (2002) 373 [arXiv:hep-ph/0206241].
- [37] A. Krämer and H. G. Dosch, Phys. Lett. B **252** (1990) 669.
- [38] A. Krämer and H. G. Dosch, Phys. Lett. B **272** (1991) 114.
- [39] H. G. Dosch, E. Ferreira and A. Krämer, Phys. Lett. B **289** (1992) 153.
- [40] H. G. Dosch, E. Ferreira and A. Krämer, Phys. Rev. D **50**, 1992 (1994) [arXiv:hep-ph/9405237].
- [41] H. G. Dosch, Phys. Lett. B **190** (1987) 177.
- [42] H. G. Dosch and Y. A. Simonov, Phys. Lett. B **205** (1988) 339.
- [43] Y. A. Simonov, Nucl. Phys. B **307** (1988) 512.
- [44] O. Nachtmann, Annals Phys. **209** (1991) 436.
- [45] A. Donnachie, G. Dosch, O. Nachtmann and P. Landshoff, “Pomeron Physics And QCD,” *Cambridge University Press, Cambridge 2002*.
- [46] G. P. Korchemsky, Nucl. Phys. B **550** (1999) 397 [arXiv:hep-ph/9711277].
- [47] A. Bialas, H. Navelet and R. Peschanski, Phys. Lett. B **427** (1998) 147 [arXiv:hep-ph/9711236].
- [48] A. Bialas, H. Navelet and R. Peschanski, Phys. Rev. D **57** (1998) 6585 [arXiv:hep-ph/9711442].
- [49] C. Ewerz, arXiv:hep-ph/0306137.



- [50] R. Peschanski, Phys. Lett. B **409** (1997) 491 [arXiv:hep-ph/9704342].
- [51] L. N. Lipatov, Sov. Phys. JETP **63** (1986) 904 [Zh. Eksp. Teor. Fiz. **90** (1986) 1536].
- [52] J. Bartels, M. G. Ryskin and G. P. Vacca, Eur. Phys. J. C **27** (2003) 101 [arXiv:hep-ph/0207173].